Evaluation of Translocation Properties of a Gut-on-a-Chip Intestinal Barrier Model

Samuel Confederat

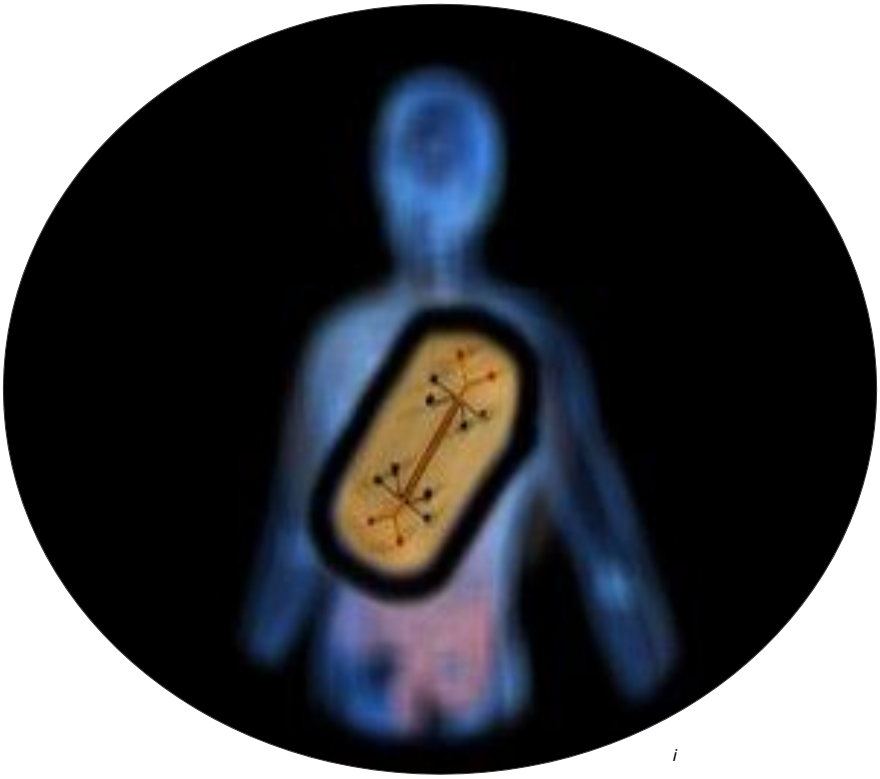

i

Wageningen, 2016

RIKILT WAGENINGEN UR

HZ UNIVERSITY OF APPLIED SCIENCES

Evaluation of Translocation Properties of a Gut-on-a-Chip Intestinal Barrier Model

Final thesis report

In-company supervisor: Dr M. van der Zande

In-school supervisor: Dr J. M. de Winter

HZ University of Applied Sciences Vlissingen

Department: Chemistry

Place of publication: RIKILT, Wageningen

Date of publication: 12.06.2016

Academic year: 2015-2016

i Retrieved from Whyss Institute, 2016: http://wyss.harvard.edu/viewmedia/109/lungonachip-microdev

Abstract

Microfluidic devices have the potential to adopt more accurate physiological conditions of the human intestine through the use of continuous flow and by producing mechanical stress to the cells. This study evaluated the translocation properties of a microfluidic gut-on-chip device in comparison with conventional static Transwells. The dynamic *in vitro* model consisted of a microchip with a porous membrane assembled and connected to a syringe pump system. This allowed for constant flows to be streamed through the apical and basolateral side of the membrane, thereby feeding the cells with fresh medium and producing mechanical shear stress. Antipyrine, a highly permeable model drug, was used to investigate the translocation across Caco-2 intestinal cells, together with a low permeability marker, Lucifer Yellow, commonly used to assess the monolayer integrity. The results showed comparable permeability coefficients in the two *in vitro* models. The translocation of Antipyrine revealed a similar linear transport trend in Transwell inserts and gut-on-chip. The apparent permeability (P_{app}) was found to be relatively higher in the Transwell inserts when compared to the gut-on-chip, with 17.4 x 10^{-6} cm s^{-1} P_{app} determined under static conditions, and 7.59 x 10^{-6} cm s^{-1} in the case of the dynamic microchip. Well-formed tight junctions, characteristic of differentiated Caco-2 cells, were suggested by permeation of Lucifer Yellow, revealing insignificant amounts translocated across the Caco-2 monolayer upon a 24hr exposure time. The P_{app} values determined for Lucifer Yellow correlated well in the two *in vitro* models, with 0.94 x 10^{-6} cm s^{-1} computed in Transwell inserts, and 0.60 x 10^{-6} cm s^{-1} in the gut-on-chip, respectively. These findings support the validity of the gut-on-chip device, indicating consistent permeability results relative to the well-studied Transwell systems. Furthermore, the use of gut-on-chip showed advantages in obtaining more automatised conditions and a minimal consumption of reagents. Nevertheless, further experiments are required for a more detailed picture of the gut-on-chip and its feasibility for translocation studies, given the limited experiments performed on this device, as compared to the static model.

Acknowledgements

I would like to express my appreciation to the people that helped me throughout this project. First of all, I would like to thank Dr Meike van der Zande and Dr ir Hans Bouwmeester for giving me the opportunity to perform my thesis project in their research group at RIKILT. I was given the opportunity to work on an interesting and challenging project that helped me gain extensive knowledge and research competences. Their guidance and constructive feedback had a significant impact on the progress of my project.

I am heartily thankful to Kornphimol Kulthong for her assistance in my daily lab work and for the great enthusiasm and patience showed during my time spent at RIKILT. Moreover, my compliments also go the members of the Nanotoxicology group for sharing their expertise during our group meetings and in the lab, but also for the warm welcome given.

Lastly, I would like to thank my in-school mentor Dr José de Winter for her great support, advice and efficient communication throughout this project.

Table of Contents

Abbreviation list

ACN	Acetonitrile
ANT	Antipyrine
DMEM	Dulbecco's Modified Eagle Medium
DMSO	Dimethyl Sulfoxide
EDTA	Ethylenediaminetetraacetic Acid
HPLC	High Performance Liquid Chromatography
LY	Lucifer Yellow
MeOH	Methanol
LOD	Limit of Detection
LOQ	Limit of Quantification
Mili-Q	Ultrapure Water
MTT	3-(4,5-Dimethylthiazol-2-yl)-2,5-Diphenyltetrazolium Bromide
NEEA	Near Essential Amino Acids
P_{app}	Apparent Permeability
P-gp	P-glycoprotein
SD	Standard Deviation
TEER	Transepithelial Electric Resistance
TFA	Trifluoroacetic Acid
UV	Ultraviolet

1. Introduction

The intestinal epithelium acts as a gatekeeper for the human body, controlling the entry of various nutrients and xenobiotics. The absorption at the gastrointestinal level is known to be of highly complex nature, posing many challenges when it comes to understanding the translocation and metabolism of substances. For this reason, considerable efforts have been dedicated to develop *in vitro* models that are able to mimic the conditions present in the human intestine, being of great relevance in the field of pharmaceuticals and nutrition. Most of the prediction models for the study of oral absorptive processes rely on culturing cell lines based on human intestinal epithelial cells, such as Caco-2 cells, on Transwell systems. Various static *in vitro* models are available for translocation studies, where the compound is added to apical side and allowed to permeate through the monolayer to the other side (basolateral). These models, however, cannot fully capture the intricate complexity found *in vivo* (i.e. intraluminal fluid flow, surface-to-liquid ratios, microvilli structures) [1] [2]. Therefore, it has been hypothesised that the use of dynamic *in vitro* models can lead to a more accurate simulation of the human intestinal absorption.

One way to achieve the dynamic conditions described above is through miniaturization. At RIKILT-Wageningen University a microfluidic gut-on-a-chip model has been developed recently. The microfluidic prototype consists of two sub-compartments (apical and basolateral side) separated by a porous polyester membrane on which cells are grown. A fluid flow, running through both the apical and basolateral chambers constantly refreshes the cells with medium and induces shear stress to the cells. Given the incorporation of these dynamic, human-like conditions, it is anticipated that this gut-on-chip model will lead to a faithful or improved representation of the human intestinal absorption, thereby having the potential to replace or reduce the use of *in vivo* animal models [3] [4] [5]. Nevertheless, the robustness of this new prototype for translocation studies requires a detailed examination, as the functionality of such model is poorly understood.

The main research question for this study was to investigate the translocation efficiency of a dynamic gut-on-chip microdevice in comparison to the static Transwell system, which is still considered the golden standard for *in vitro* translocation studies. To evaluate the translocation efficiency, model compounds (high and low permeability) were applied to the apical side, and measuring the concentration in the basolateral side by means of HPLC analysis. In both systems, Caco-2 cells were used as cell model for the barrier. Tasks in this project deriving from the central aim were: development of HPLC method for the selected compounds; excluding cytotoxicity of the model compounds used for translocation experiments; exposure and translocation studies using Transwells; exposure and translocation studies using gut-on-chip microdevice.

2. Theoretical framework

2.1. Human intestinal absorption

When it comes to human gastrointestinal absorption, this occurs almost entirely in the small intestine region. The small intestinal epithelium contains villi and microvilli structures that dramatically increase the surface area available for absorption and digestion mechanisms. A major function of the small intestine is the selective absorption of major nutrients, but also a barrier to certain ingested foreign substances, or digestive enzymes [6]. As for the epithelial cells in the intestinal region, these are a heterogeneous population of cells, including enterocytes and mucin-secreting cells, among others. However, the majority is represented by enterocytes, with a predominant role in the absorption of drugs and nutrients in the small intestine [7]. The enterocytes are highly polarized resulting in different properties of the apical and basolateral membranes. The cells in the intestinal epithelial are tightly connected to each other with tight junctions [7]. For the translocation of compounds two main absorption mechanisms are possible: passive diffusion (paracellular and transcellular), and active processes (carrier-mediated) [8] (Figure 1).

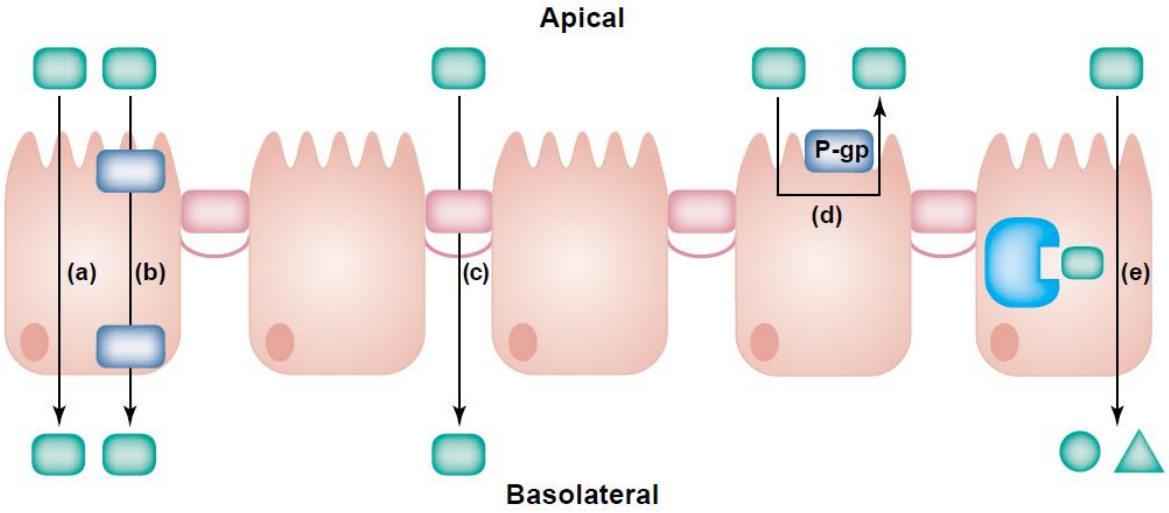

Figure 1: Schematic displaying the different routes and mechanisms of compound transport through the intestinal epithelium: **(a)** transcellular passive permeability; **(b)** carrier-mediated transport; **(c)** paracellular passive permeability. Apart from these, there are also mechanisms that can hinder absorption: **(d)** P-gp efflux transporter; and **(e)** metabolic enzymes. Adapted from Balimane *et al.* [8].

2.2. *In vitro* cell culture-based permeability models

2.2.1. Caco-2 cells

Numerous studies shed light on the development of cell culture models for intestinal absorption. Among the most extensively characterised cell model is Caco-2 cell line, considered a well-established predictor for drug permeability studies and *in vivo* bioavailability [9] [10]. Originating from the human colon carcinoma, Caco-2 cells acquire numerous features of absorptive intestinal cells during culturing, such as microvillus structure, hydrolysis enzyme, and carrier mediated systems [11]. Caco-2 cells are known to spontaneously differentiate, leading to the formation of polarised monolayers with structure resembling that of enterocytes [12] [13]. The integrity of the monolayer formed exerts an influence on permeability of molecules in the apical-to-basolateral direction. The tight junctions connecting the cells with each other also serve as a route for the paracellular movement across the monolayer [14]. Therefore, the permeability in Caco-2 monolayers is expected to give comparable results to the *in vivo* conditions. However, it should be noted that Caco-2 are derived from human colon adenocarcinoma, which brings the possibility of retaining certain colonic epithelium characteristics, as previously described in several studies [15] [16] [17]. Although Caco-2 cells express many important uptake and efflux transporters, reported differences in the expression of P-gp efflux transporter (over-expressed), and CYP3A4 (weakly expressed or absent), but also the absence of the mucus secreting goblet cells, may influence the permeability of compounds in Caco-2 cells, as compared to *in vivo* studies [18].

While Caco-2 cell line still remains the main choice for *in vitro* permeability model, recent attempts to obtain more complex representation of the *in vivo* epithelium cells involved the use of co-cultures, such as Caco-2 and HT-29 (mucin-producing goblet cells) cell lines. This model comprises the two cell lines mixed in similar proportions to those normally found *in vivo* [19], allowing in certain cases for more flexibility in adjusting to the *in vivo* conditions, as compared to using monocultures. It has been also reported that the use of such co-culture model has the potential to fill in certain gaps with regard to the compounds transported *via* the paracellular route, often underrepresented in Caco-2 monolayers [20]. Apart from this, a new alternative concerning the intestinal absorption research that is also gaining recent relevance is the use of organoids. These in vitro 3-dimensional human intestinal tissues are the result of direct differentiation of human pluripotent stem cells [21] [22]. The resulting human intestinal tissue shows comparable functions to the ones found *in vivo*, as it can secrete mucin, but also due to the presence of defined brush borders [21].

2.2.2. Static systems

The growing interest in addressing challenges related to oral absorption of nutrients and drugs stimulated the development of *in vitro* intestinal cell models, traditionally performed on cell culture systems such as 96-well plates or Transwell systems. Of particular interest is the extensive use of Transwell permeable supports. This *in vitro* model stands as a major driver in terms of studying intestinal absorption and permeability of compounds [23]. In a typical setup for permeability studies, Caco-2 cell monolayers are cultured on porous membrane incorporated in permeable plastic supports that can be fitted into multi-well culture plates, allowing test compounds to be added to the apical side and measured in the basolateral side of the monolayer (Figure 2). The use of permeable *in vitro* inserts allows cells to be grown and examined under polarised circumstances by employing normal culture conditions.

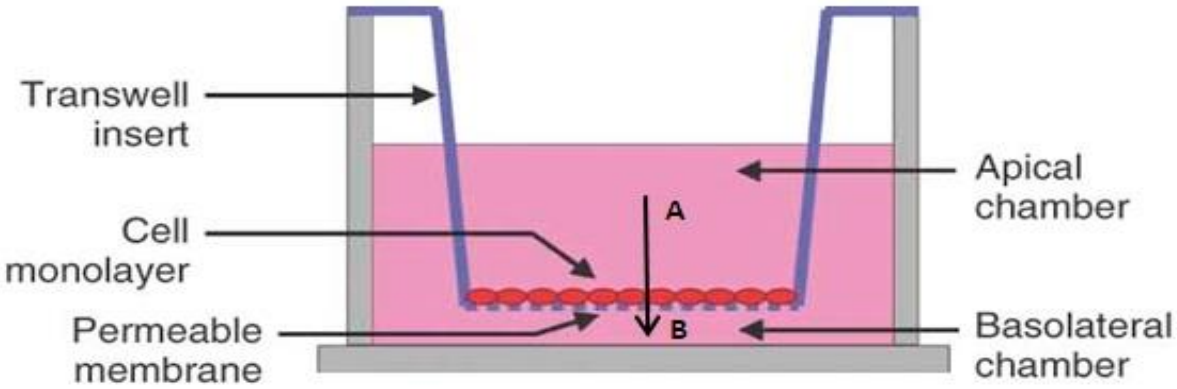

Figure 2: Transwell insert scheme portraying the separation of apical and basolateral chamber by a permeable membrane with a cell monolayer on the apical surface. Absorptive transport takes place in the A (apical)-to-B (basolateral) direction. Adapted from Brunswick Laboratories [24].

The static nature of these *in vitro* models, however, raises questions to what extent the *in vivo* conditions are simulated. Aspects ranging from lack of fluid flow, surface-to-liquid ratios, mechanical stimuli, or concentration gradients tend to generate drawbacks in capturing the *in vivo* complexity. Another deficiency of these traditional cell culture systems are the long growth times required (21 days) for the intestinal cells to reach confluence and differentiate into functional enterocytes [25]. Furthermore, it has been reported in previous studies that Caco-2 monolayers in Transwell cultures display low paracellular permeability values than those observed in human or animal *in vivo*. One theory related to this problem is that the static nature of the *in vitro* model leads to the formation of a thick unstirred fluid layer which can infringe the diffusion process [26] [27]. A second speculative explanation for the discrepancy showed in the paracellular permeability in Caco-2 monolayers could be associated to differences in the control of tight junction permeability and the water fluxes in the cell monolayers [28] [29] [30]. Moreover, limitations have been proposed to come from the high expression of P-glycoprotein, which may lead to elevated secretion rates, and consequently to lower permeability in the absorptive direction [20] [31].

2.2.3. Dynamic systems

Recent advancement in microfluidics and bioengineering led to the development of "organs-on-chip" prototypes [4] [32] [33]. These novel modes have the potential to reproduce more accurately the *in vivo* complex microenvironment. Several gut-on-chip prototypes have emerged in the recent years [34] [35] [36] [37]. The gut microfluidic system simulates the low fluid flow and shear stress experienced, typical of *in vivo* conditions. The microenvironment can also regulate the ratio of cell number to medium volume in order to keep sufficient concentrations of metabolic products in the medium, one major factor that is missing in the static culture models. Kim *et al.* [35] reported a "human gut-on-a-chip" microdevice containing intestinal epithelial Caco-2 cells cultured on a porous membrane. In this setup, a low flow of 30 μl h^{-1} was integrated, producing low shear stress on the cells, but also cyclic strain that simulated the human-like peristaltic motions. Their studies demonstrated well-defined epithelial monolayers formed within three days under these conditions, much faster than what was obtained in conventional cell culture systems, which normally requires up to 21 days of culture to achieve similar cell morphology. Comparable results have been reported also in the study conducted by Imura *et al*. [34]. What is more, their dynamic microfluidic model showed a significant potential for highly sensitive and effective application for the analysis of drugs and chemicals [34]. Furthermore, the use of such dynamic model stands as a potential platform for testing different co-cultures, or relevant microbes. In this sense, the study performed by Ramadam *et al.* [36] explored the effects of dairy products on the immune functions in the gastrointestinal tract using microfluidic intestine-on-a-chip model.

3. Materials & methods

3.1. Reagents & chemicals

Analytical standard Antipyrine, together with Lucifer Yellow were purchased from Sigma-Aldrich (The Netherlands). DMSO was obtained from J.T. Baker (The Netherlands) and Ethanol from Klinipath B.V. (The Netherlands). HPLC grade acetonitrile and methanol were purchased from ACTU-ALL Chemicals (The Netherlands), whereas TFA was obtained from Thermo Scientific (The Netherlands). A MilliQ system (ELGA) was used to prepare deionised water for HPLC mobile phases and sample preparation.

3.2. Cells and culture conditions

Human intestinal epithelial Caco-2 cell line (HTB-37) was obtained from ATCC (American Type Culture Collection) and it was used between passage 28 and 41. The cells were grown in Dulbecco's Modified Eagle Medium (DMEM; Bio Wittaker) containing 4.5 g/L Glucose with L-Glutamine, supplemented with 10% heat inactivated fetal bovine serum (FBS; Gibco), 1% mixture of streptomycin and penicillin (Gibco), and 1% near essential amino acids (NEAA; Gibco). Cells were grown at 37°C in a humidified incubator (95% relative humidity) under 5% CO_2 atmosphere. Routine passaging of cells stocks was carried out in 75 cm^2 flasks (Costar). For sub-culturing, the cells were trypsinised with a solution containing 0.25% Trypsin (w/v) and 0.09% (w/v) EDTA.

3.2.1. Transwell culturing

For the conventional static 12-well Transwell system (Corning Costar), Caco-2 cells were seeded at 300,000 cells/ml on porous polyester membrane inserts (1.12 cm^2 surface area, 0.4 µm pore size). Culture medium was refreshed every other day on both the apical (0.5 ml) and basolateral side (1.5 ml) of the Transwell cell culture insert throughout the 21 days post-seeding period.

3.2.2. Microdevice design & on-chip culturing

The microfluidic chip (Micronit, The Netherlands) consisted of two resealable glass slides that were assembled with a cell culture membrane sandwiched between them to form an upper and lower flow chamber (Figure 3A). The upper and lower channels had the same size (0.25 mm high X 11 mm wide), with the porous polyester membrane in between (area 1.0 cm^2, 0.40 µm pores). This allowed the flow of two different fluids, on either side of the membrane. A dual syringe pump system (PE-4000 QIS) was used to generate a constant flow in the apical and basolateral channel of the microchip, connected to the syringe needle *via* capillary tubes (Figure 3C). During the culturing time, the microfluidic system was kept in an incubator at 37◦C.

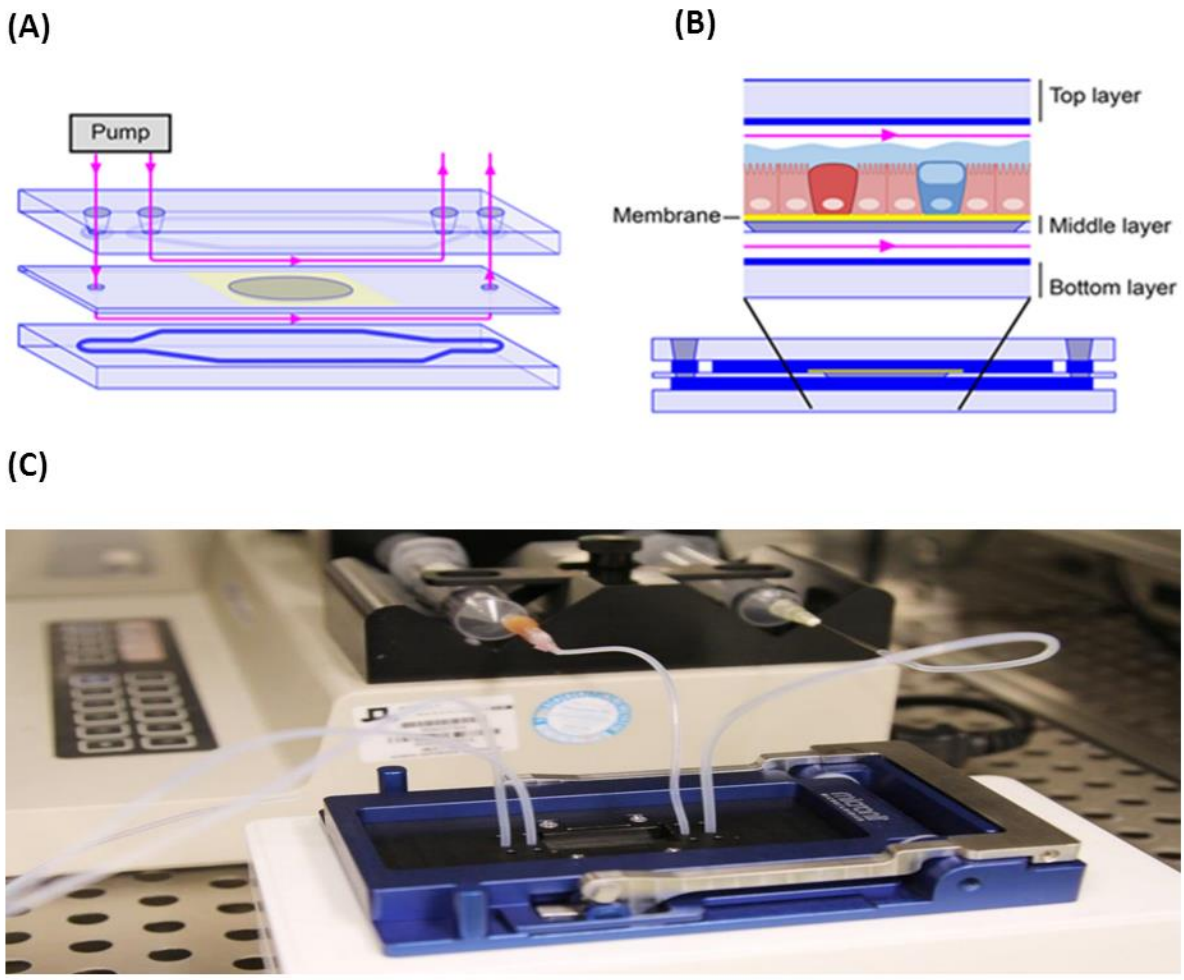

Figure 3: The gut-on-chip dynamic model. **(A)** Schematic of the microfluidic chip pumped through the microchannels in the direction indicated by the arrows. **(B)** Cross-section displaying the internal layers of the microdevice. **(C)** Photograph of the microfluidic device connected to the syringe pump system with two separate syringes streaming fluid through the upper and bottom channel. At the outlet side of the chip, two tubes were connected to facilitate the sample collection from each channel.

Prior to seeding, the microchip assembly was sterilised by perfusion with 70% (v/v) ethanol, followed by a rinse with culture medium. Caco-2 cells were seeded on the microchip similarly to the procedure performed in Transwells. After seeding the cells (300,000 cells/ml) onto the porous membrane, the chip was incubated overnight at 37°C in a humidified incubator with 95% relative humidity, under 5% CO_2 atmosphere, to allow the cells to attach onto the membrane. Following the overnight incubation, the chip was prefilled with medium and assembled into the chip holder connected to the syringe pump system. The Caco-2 cells were cultured for 6 days with continuous medium being perfused through the upper and lower channel at a constant flow rate of 30µl h^{-1}.

3.2.3. Epithelial barrier measurements

The monolayer formation was assessed by measurements of the transepithelial electric resistance (TEER). This parameter was measured three times per week during the 21 days culturing in Transwell inserts. During the procedure, the cell culture medium was changed before each TEER measurement. TEER was determined using a Millicell-ERS device (Millipore) and chopstick-style electrodes. Mean TEER values of three wells were calculated per passage. TEER values were calculated by subtracting the resistance (in Ohms) of a blank insert (cell-free) from the recorded resistance of the cellular monolayer, and multiplying by the available surface area of the insert's membrane.

3.3. Viability assay

Caco-2 cells were seeded on 96-well plates at 75,000 cells/well. MTT (Thiazoyl Blue Tetrazolium, Sigma) was used to assess cell viability. The principle of this assay is based on the metabolism of tetrazolium colourless salt to a blue formazan by viable cells, with the measured absorbance being proportional to the amount of viable cells. After 24hr of incubation in presence of the drug, Antipyrine (0.0-2.0 mg/ml), 100 µl of MTT solution (1.0 mg/ml) was added to each well and incubated for 3hr. Subsequently, 100 µl DMSO was added to the wells to solubilise the formazan formed in the viable cells. After 10 min of stirring, the absorbance was measured using a Microplate reader (Bio-Tek) at 540nm. Triplicates were used for each compound tested, together with negative (medium) and positive (0.1% Triton-X 100) controls. Consequently, cell viability was calculated as a percentage of the mean of the negative cell culture.

3.4. Translocation experiments

Translocation studies for Antipyrine and Lucifer Yellow (Table 1) were performed in Transwells at day 21 post-seeding, following the examination of monolayer integrity of each culture insert by TEER measurement. Working solutions were prepared in culture medium (DMEM). Translocation studies were conducted in triplicates at three different passages. Antipyrine was investigated at a concentration of 1.0 mg/ml, whereas Lucifer Yellow, the low permeability marker used to monitor the monolayer integrity, was used at a concentration of 0.5 mg/ml. Blank measurements containing culture medium without the test compound were included.

Table1: Characteristics of the model compounds used for translocation studies.

Compound	MW (g/mol)	Permeability	Transport
Antipyrine (ANT)	188.23	High	Passive, transcellular route [38]
Lucifer Yellow (LY)	444.24	Low	Passive, paracellular route [39]

Permeability experiments were initiated by adding 0.5 ml of culture medium containing the compound to the apical chamber and 1.5 ml culture medium to basolateral chamber. Subsequently, the Transwell sets were incubated at 37°C in a humidified incubator (95% relative humidity) under 5% CO_2. After 15, 30, 60, 90, and 120 min, 0.2 ml sample was withdrawn from the basolateral compartment and replenished with an equal volume of culture medium. Ultimately, after 24hr incubation, samples from both apical and basolateral side were collected for mass-balance calculation. The collected samples were pre-treated with 2:1 volume of ACN/MeOH mixture (50/50) and centrifuged for 10 min at 10,000 rpm, 4°C and the supernatant was used for HPLC analysis. Fluorescence measurements of LY compound were determined by using a Microplate Reader Bio-Tek. Samples (50µl) were transferred to a 384-well black plate (BRAND; Germany) and fluorescence measured at 485 nm excitation wavelength and 530 nm emission wavelength.

3.5. HPLC analysis

Samples from the translocation experiments of ANT were analysed by means of High Performance Liquid Chromatography (HPLC) coupled to an UV detector to quantify the amount of compound present in the aliquots collected at different time points. The HPLC system consisted of a binary PE Flexar pump with an on-line degasser, PE Flexar column compartment, a PE Flexar autosampler, and a PDA detector PE Flexar. Samples (50 µl) were injected onto a C18 reverse-phase column (4.6x150 mm, 5 µm) with a guard column attached (4.6x7.5 mm, 5 µm) (Alltech, The Netherlands). The mobile phase consisted of 0.1% TFA in Milli-Q water (A), and HPLC-grade Acetonitrile (B). For the analysis of ANT a linear gradient was applied. The elution conditions were initiated at 10% B increasing in 20 min at 100% B, following a return to the initial conditions in 2 min, and a 10 min post-equilibration. The flow rate was maintained at 1.0 ml/min throughout the entire analysis time. The column temperature was set at 25°C. Calibration lines (n=3) were included for the quantification of the compound.

3.6. Data analysis

Adopting the model previously described by Lemiuex *et al.* [40], the apparent permeability coefficient (P_{app}) for each compound was calculated as follows:

$$P_{app} = \frac{dQ}{dt} \times \frac{1}{AC_o}$$

where dQ/dt represents the amount of compound transported per time point (mg s^{-1}), A is the surface area of the filter (cm^2), and C_0 is the initial donor concentration (mg/ml). In order to compute dQ, the amount of compound, for 30, 60, 90, and 120 min time point, a correction was required to account for the removal of the sample from basolateral side at earlier time points.

The mass balance (R) was calculated as:

$$R(\%) = 100 \times \frac{A + D}{D_0}$$

with A and D being the amounts of analyte in the acceptor (basolateral) and donor (apical) sides, respectively. Whereas D_0 is the amount introduced at the start. Every experiment was repeated three times, with triplicates for each condition. The results are represented as mean of ± SD.

4. Results & discussion

4.1. Cytotoxicity results

The first step prior to the translocation experiments was to define suitable non-cytotoxic concentrations for the model compounds applied. In this sense, the MTT assay was used to assess cell viability at a defined concentration range of the compound. Caco-2 cells (one day post-seeding) were exposed to ANT prepared in DMEM in the 0.0-2.0 mg/ml concentration range. As shown in Figure 4, the results obtained by MTT assay led to a decrease in cell viability (>80%) at a dosage higher than 1.0 mg/ml, whereas at 1.0 mg/ml the cell viability was found to be approximately 86% (Figure 4). It was concluded that ANT was non-cytotoxic at a concentration lower than 1.0 mg/ml. Based on these results, 1.0 mg/ml was chosen as a suitable concentration for translocation studies, being a good comprise between cell viability and analytical detection for the HPLC quantification. The cytotoxicity was assessed using undifferentiated cells, whereas the final translocation experiments were performed using differentiated, mature Caco-2 cells following a 21 days culturing period. It has been established before that undifferentiated cells show higher sensitivity upon exposure than differentiated cells [41]. Thus, the cytotoxicity results can be regarded as worst-case experiments.

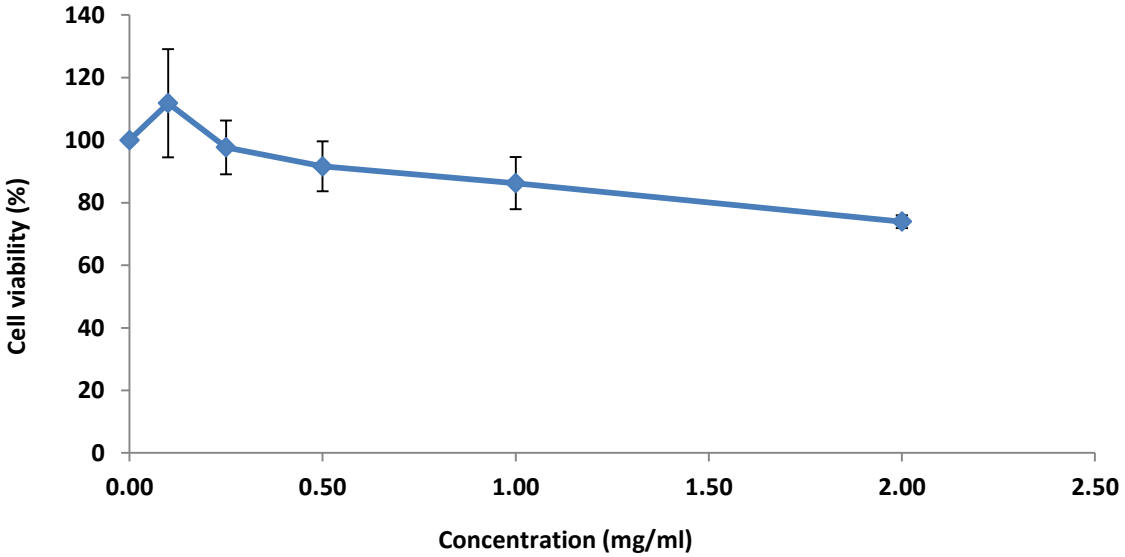

Figure 4: Antipyrine cytotoxic effect on Caco-2 culture upon exposure to 0.0-2.0 mg/ml concentration range. Cell viability, presented as mean±SD (n=3), was assessed by MTT assay at 3 different passages.

4.2. HPLC method development

An HPLC method was developed for the analysis of ANT, adopting chromatographic conditions previously described by Li *et al.* [42]. The chromatographic peak for ANT in DMEM solution occurred at 6.6 min (Figure 5A), with the optimum UV detection wavelength set at 230nm. Given the hydrophilic nature of ANT compound, this was completely dissolved in DMEM at 1.0 mg/ml, without any prior usage of additional solubiliser. For the HPLC analysis of ANT in DMEM a pre-treatment step was applied in order to remove potential proteins and lipids present in the medium. This was done by adding 2:1 volume of ACN/MEOH mixture (50:50), followed by centrifugation at 10,000 rpm for 10 min, at 4 ◦C, with the resulting supernatant being injected onto the HPLC. No significant interfering chromatographic peaks were observed in the retention time window of the analyte when blank samples (only DMEM) were analysed (Figure 5B).

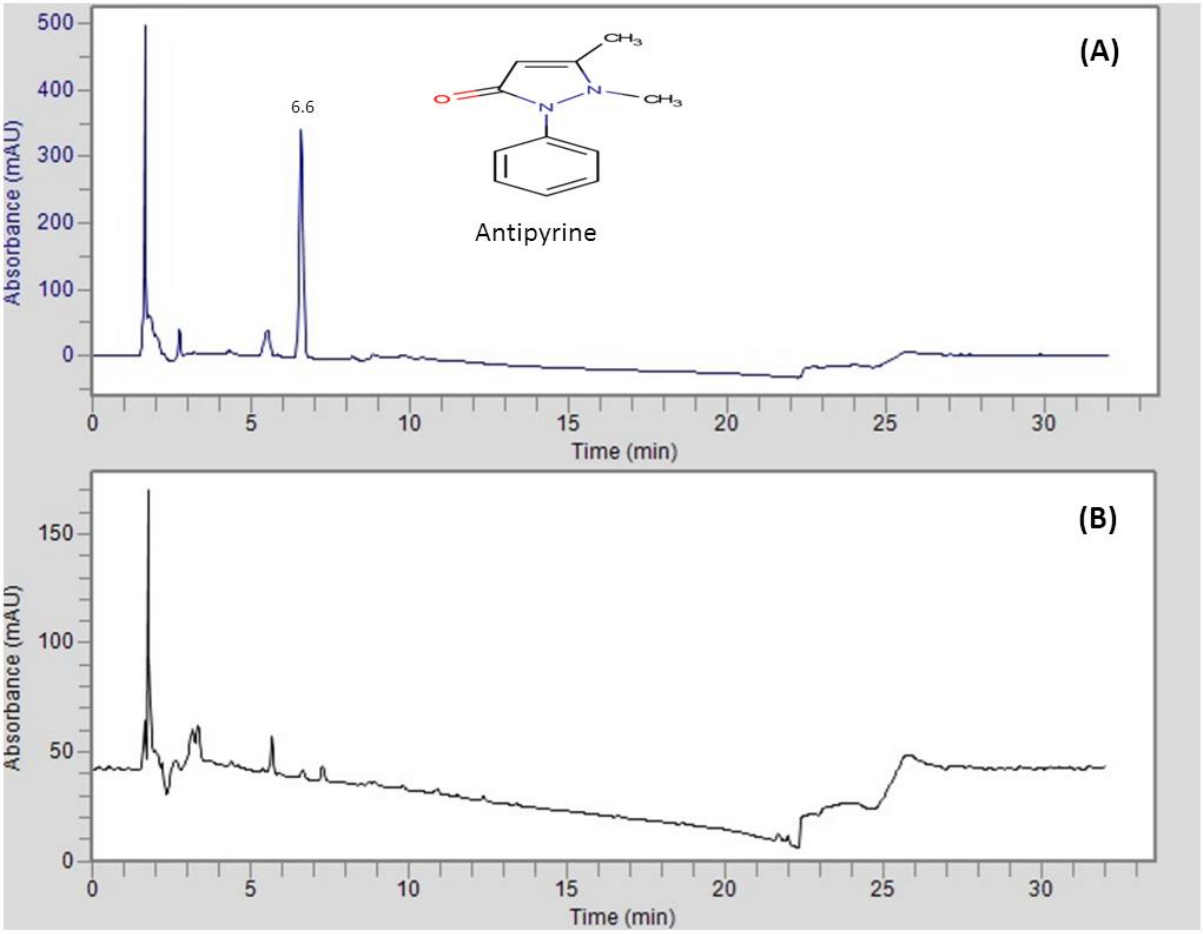

Figure 5: Representative HPLC chromatographs for (**A**) ANT (0.1 mg/ml) prepared in DMEM, and (**B**) DMEM blank sample. Separation was achieved on a C18 column (4.6x150 mm, 5 µm) with a guard column attached (4.6x7.5 mm, 5 µm). 0.1%TFA (solvent A) and ACN (solvent B) were used as mobile phase components. Flow rate was set at 1.0 ml/min. The ANT peak eluted at 6.6 min following a linear gradient, with a detection wavelength set at 230 nm. Data processed using PE Chromera software.

4.2.1. Recovery and stability

Following the method development for the analysis of ANT, additional measurements were performed to investigate the recovery of ANT in DMEM after the protein precipitation step. For this purpose, spiked samples of 0.1 mg/ml ANT were prepared in MilliQ and DMEM and analysed by HPLC. The results showed a 87±4% (n=3) mean extraction recovery of ANT from DMEM, relative to the results in MilliQ, suggesting that minimal amounts of compound are lost during DMEM protein precipitation step with ACN/MeOH mixture (Appendix 2, Figure 14A). In addition to this, the compound stability when incubated at 37◦C in DMEM was investigated, simulating the actual conditions during translocation experiments. The results indicated that no less than 99±5% (n=3) of ANT remained in the solution after 24hr incubation at 37◦C in DMEM (Appendix 2, Figure 14B).

4.2.2. Range and linearity

As far as the ANT quantification is concerned, calibration graphs (n=3) were constructed in the 0.005 to 0.5 mg/ml range (Table 2) by plotting the analyte concentration against peak area. For the calibration graph, spiked samples in DMEM of six different concentrations were used to cover the quantitative range. The constructed calibration line for ANT showed a very good linearity, resulting in a correlation coefficient (r^2) higher than 0.990 (Figure 6). The sample collection of ANT in the *in vitro* models permitted the use of 50 µl for injection into the column, therefore improving the analytical sensitivity of the method.

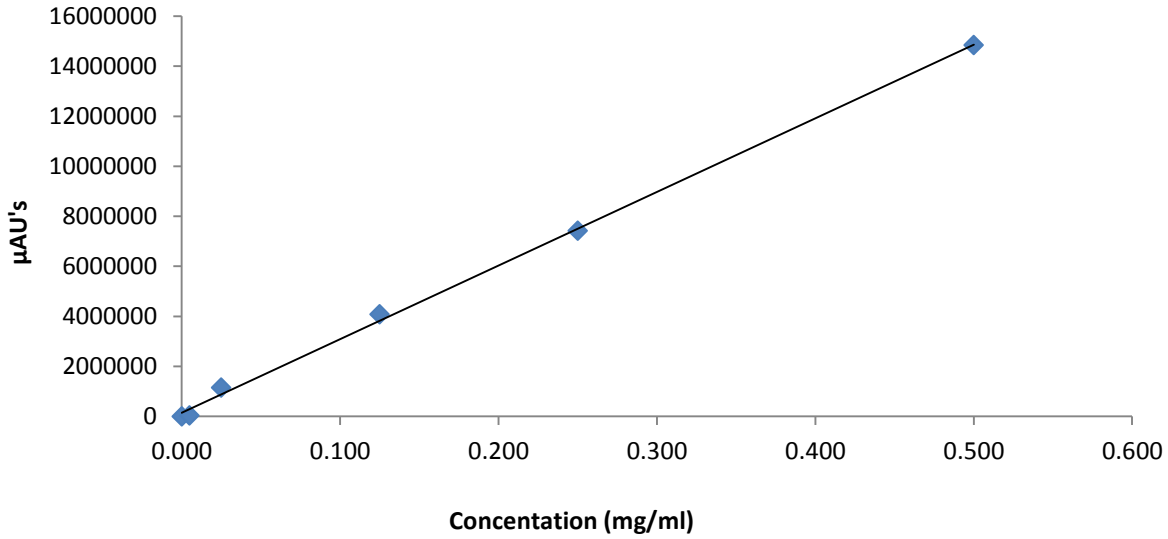

Figure 6: Calibration line of ANT prepared in DMEM in the 0.005-0.5 mg/ml range with the concentration (mg/ml) plotted against peak area (µAu's). A correlation coefficient (r^2) of 0.9986 was obtained, denoting a good linearity of the calibration graph.

Table2: Method parameters for the analysis of ANT by means of HPLC.

Parameter	**Antipyrine**
Detection wavelength	230 nm
Range (mg/ml)	0.005-0.5
Slope (Mean±SD)	30512588 ± 1962093
Intercept (Mean±SD)	134690 ± 73491
Regression coefficient	0.9986
LOD (mg/ml)	0.0005860
LOQ (mg/ml)	0.001953

Values reported as mean±SD of n=3 calibration curves, across the same linear range.

4.2.3. Limit of detection and limit of quantification

In terms of sensitivity of the HPLC method developed, this is represented by the determination of limit of detection (LOD) and limit of quantification (LOQ). LOD portrays the lowest detectable concentration of the compound using the proposed method, whereas LOQ stands for the lowest concentration of the compound that can be reliably quantified. In this sense, LOD and LOQ were computed according to the guidelines recommended by ICH [43], with LOD=3σ/S and LOQ=10σ/S (σ- SD of blank response of ≥20 replicates; S- slope of calibration curve). For the chromatographic conditions developed for the analysis of ANT, the calculated LOD was 0.0005860 mg/ml and 0.001953 mg/ml for LOQ, respectively (Table 2).

4.3. Transwell translocation studies

4.3.1. Monolayer integrity assessment

In the static model, the Caco-2 cell monolayer formation in Transwell inserts was assessed by means of TEER measurement, as an estimate of the tight junctions integrity. This was performed 2-3 times per week during the 21 days culturing period. Caco-2 cells grown on polyester Transwell inserts showed a gradual increase in TEER value over time, with maximal values obtained within two weeks culture time, reaching a steady increase in the last week of culturing. The Caco-2 monolayers displayed high TEER values (~ 1000 $\Omega.cm^2$) (Figure 7), indicating well-formed tight junctions. Nonetheless, a significantly high discrepancy in TEER values was observed between the three passages used (passage 39, 40, and 41) after two weeks culture time, depicted by the high SD showed in Figure 7. This was assumed to be as a result of potential differences in the cell density seeded on the Transwell inserts, which can lead to variations in the monolayer formation, but also different growth rates of the different passages used. Moreover, given the heterogeneous character of the Caco-2 HTB-37 cell line used in this study, differences in the TEER values has been previously described as a result of mosaic pattern in the differentiation degree of subpopulations at different passages [23]. It has been also postulated that TEER measurements do not provide a sensitive reflection of the cell membrane integrity, often being used in conjunction with a low permeation marker as additional control [44]. This can also be supported by the relatively small SD obtained for the permeation of LY at the three different passages in Transwells (section 4.3.2.), as compared to the high SD for the TEER results.

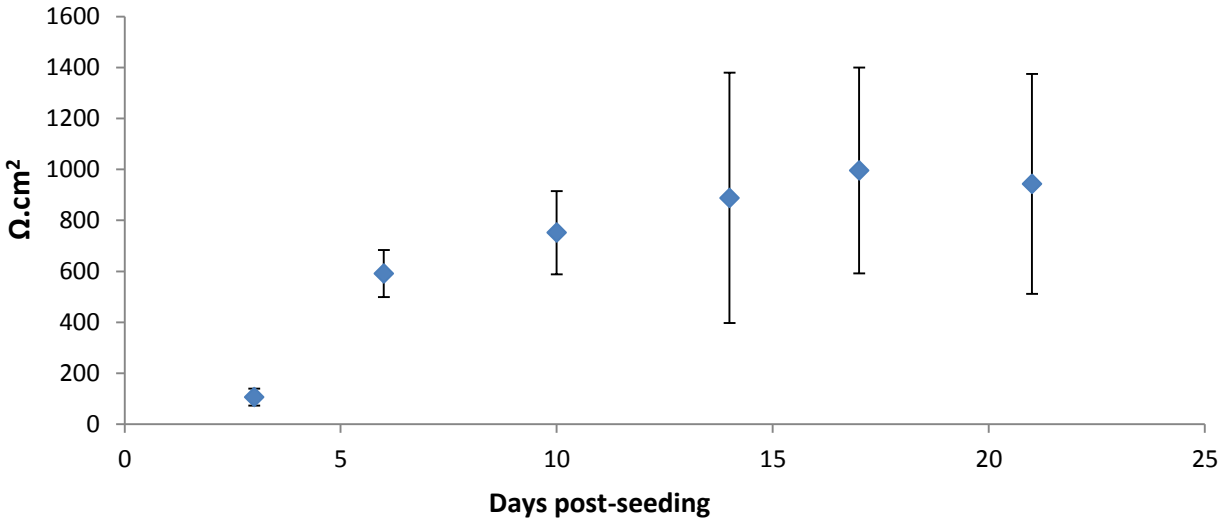

Figure 7: Integrity of the tight junctions of the Caco-2 monolayer quantified by TEER measurements. TEER measurements were performed at three different passages in triplicate, with TEER values plotted as mean±SD (n=3) over a span of 21 days culture in Transwell inserts. TEER measurements were performed before and after treatment with LY and ANT, with no significant changes in TEER, indicating that no damage to the Caco-2 cells occurred during the 24hr treatment.

4.3.2. LY translocation assay

The permeation of LY, a low paracellular permeability marker, was investigated on Transwell inserts, following the 21 days culturing period. This was applied on both inserts with differentiated Caco-2 cells and cell-free Transwell inserts in which the transport was investigated for a period of 120 min, followed by a 24hr treatment with the low permeability marker. The collected samples were quantified by measuring fluorescence intensity with the use of a Microplate reader at 485/530 nm. Figure 8A shows the transport of LY over time, demonstrating that only a low fraction of LY was transported in the BL side, with the BL amount of LY reaching a steady state (constant, unchanged movement through the membrane), after approximately 1hr exposure time. This was also in agreement with the comparison between the BL and AP amount after 24hr treatment with LY (Figure 8B), which showed that only a minute fraction of LY translocated through the Caco-2 monolayer in the basolateral part (2±1%), whereas the apical compartment showed 82±5% remained after 24hr exposure in the Transwell insert. These results, comprising a very low translocation of LY compound, denoted a good integrity of the Caco-2 monolayer integrity upon 21 days culture in Transwell inserts, behaving according the norms previously described for the permeation of LY on 21 days differentiated Caco-2 cells [45] [46].

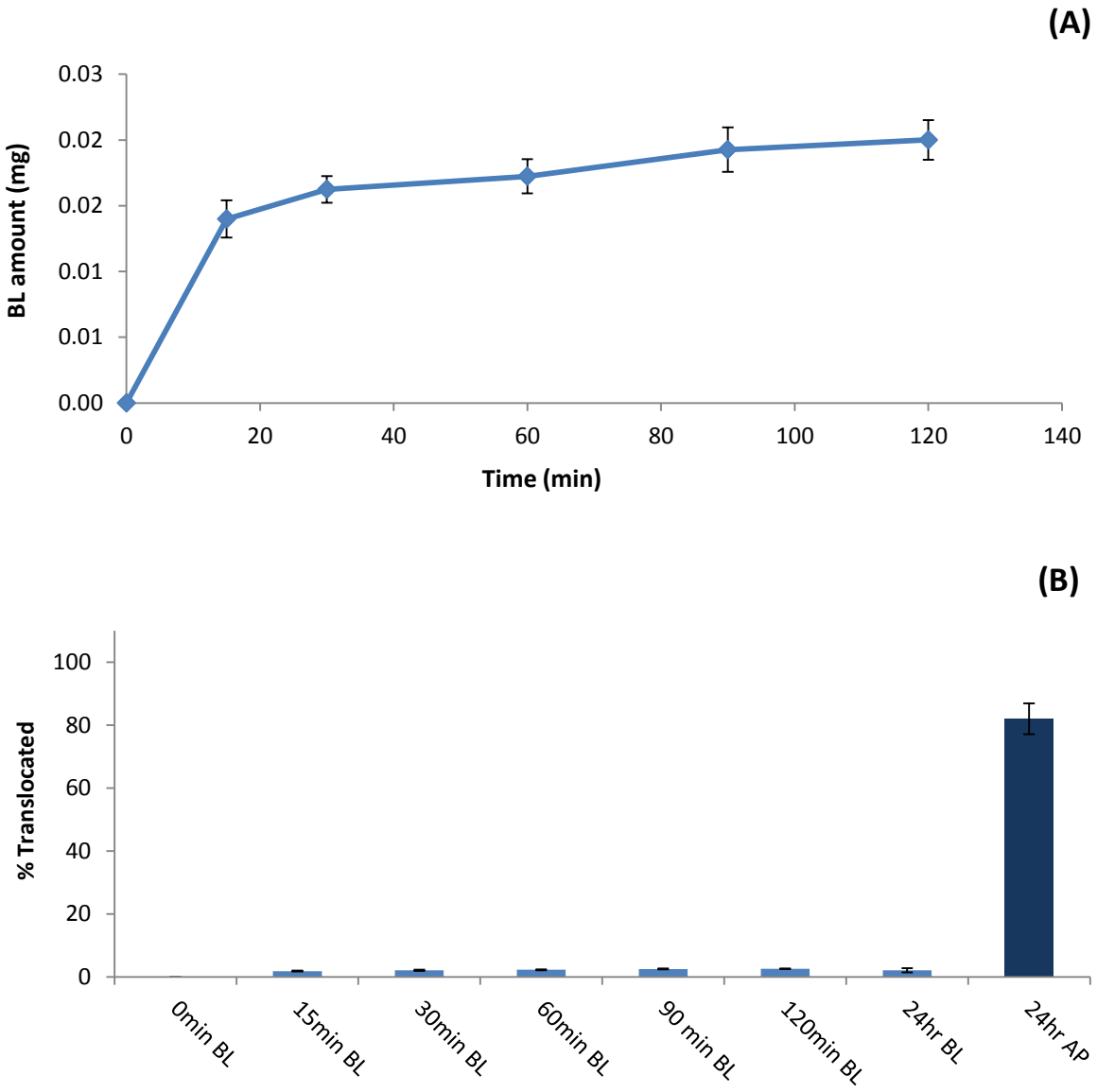

Figure 8: (A) LY transport in the apical-to-basolateral direction measured over a span of 120 min. **(B)** Bar charts representing the percentage of LY translocated through the Caco-2 monolayer over time in Transwell inserts in the BL part (light blue bars), and the remaining percentage of LY compound in the AP side after 24hr exposure (dark blue bars). Data computed as mean±SD (n=3) performed at 3 different passages (see Appendix 3 for LY calibration line).

Apart from the exposure of LY to grown Caco-2 cells, a control test was performed in Transwell inserts without cells, adopting the same transport conditions. In this case, the transport of LY across the polyester membrane showed a linear increase over time (Appendix 4), with 31±2% of LY compound translocated in the basolateral compartment, much higher than what was observed in the conditions with grown Caco-2 cells. Furthermore, the 24hr comparison between apical and basolateral compartment in the LY cell-free Transwell inserts indicated a potential adsorption of the compound to the surface material of the membrane, since only 55% of the initial amount was determined (adding up the BL and AP percentage) after 24hr exposure. This could also provide an explanation for the remaining fraction lost during LY translocation in the Caco-2 cells Transwell inserts, but also not excluding the possibility of the compound to be retained in the cell monolayer.

4.3.3. ANT translocation assay

The translocation of ANT across Caco-2 monolayer cultured on Transwell inserts was assessed upon exposure to a concentration of 1.0 mg/ml prepared in DMEM. Translocation was investigated under static conditions, with samples collected from the basolateral compartment and quantified by HPLC. The determined amount of ANT in the basolateral revealed a linear increase over time (Figure 9A), characteristic behaviour of highly permeable compounds, with 14±3% of the compound translocated in 120 min, and 33±3% ANT translocated after 24hr exposure (Figure 9B). Furthermore, the 24hr treatment with ANT led to a 21±1% of ANT remaining in the apical compartment. A striking observation, however, was the unmatched percentage of ANT translocated in the BL compartment and the ANT percentage remaining in the AP compartment. In this case, only 51% relative to the initial concentration was determined. This implied that a significant proportion of the compound was trapped inside the cells and/or to the insert membrane during the ANT exposure. However, in order to confirm these assumptions, additional experiments are required by measuring the amount of ANT in the cells following a cell lysis procedure, but also by performing translocation experiments of ANT in cell-free inserts over the same time span.

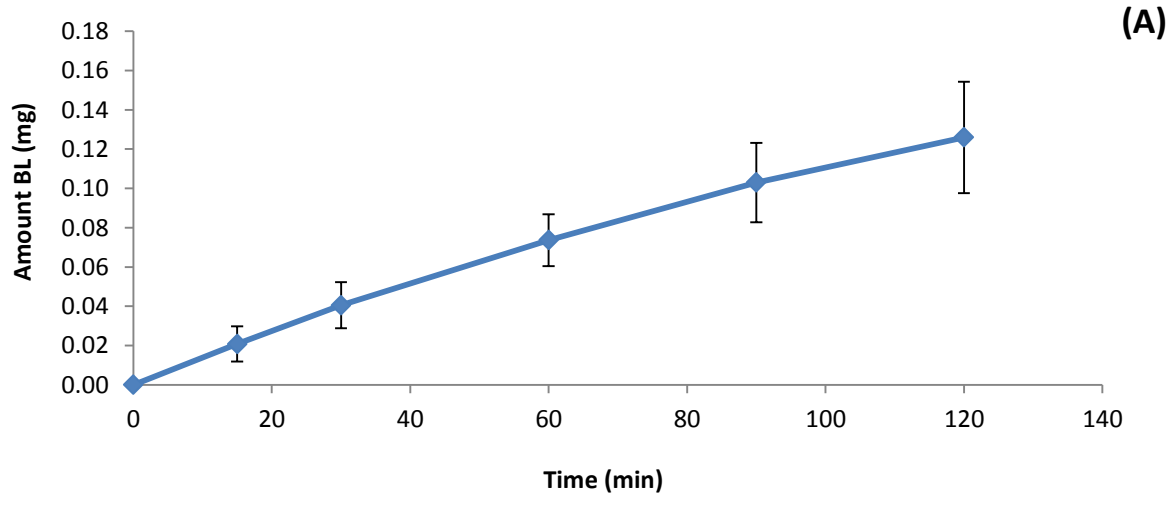

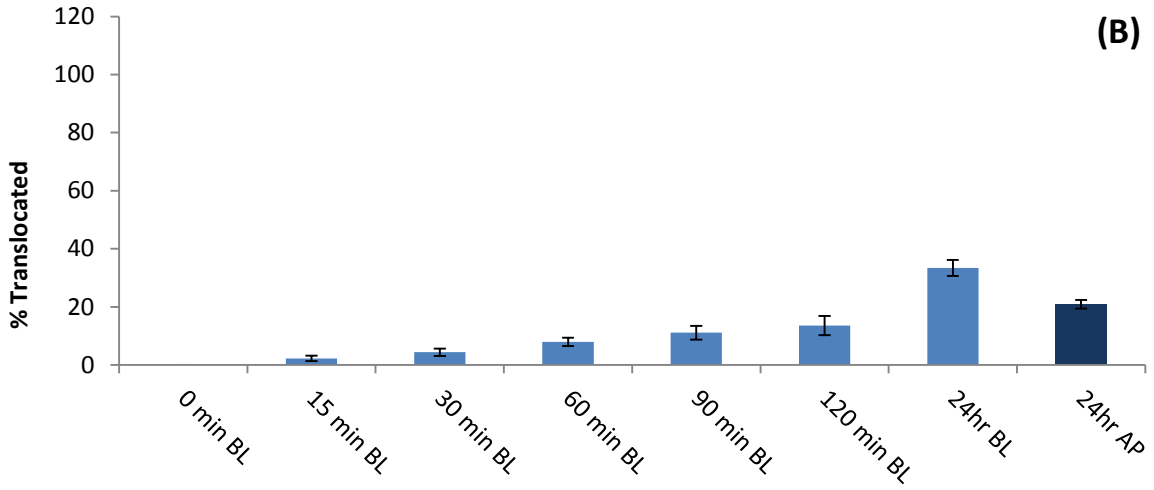

Figure 9: (A) ANT transport in the apical-to-basolateral direction measured over a span of 120 min. **(B)** Bar charts representing the percentage of ANT translocated through the Caco-2 monolayer over time in Transwell inserts in the BL part (light blue bars), and the remaining percentage of ANT compound in the AP side after 24hr exposure (dark blue bars). Data computed as mean±SD (n=3), performed at 3 different passages.

4.4. Gut-on-Chip translocation studies

The second *in vitro* cell-based model employed in the translocation evaluation of Caco-2 intestinal cells was a microfluidic gut-on-chip device. This *in vitro* model comprised of a microfluidic setup that allowed exploring the physiological conditions experienced in the human intestine. The dynamic, human-like conditions were simulated by growing Caco-2 cells on a porous membrane, assembled in a microchip with a top and bottom channel, and constant medium flow running through the channels, thereby refreshing and inducing shear stress to the cells. Previous in-house studies (unpublished data) revealed differentiated cells within 5-6 days when cultured on the microfluidic chip at a constant flow of 30 µl h^{-1}, with cells acquiring microvillus structures as a result of the shear stress applied, similarly to the findings reported by Kim *et al.* [47].

In the context of translocation studies using the gut-on-chip device, the microfluidic device underwent a sterilisation procedure by filling the tubes and the channels with 70% ethanol, followed by a rinse with medium before being used. Caco-2 cells were seeded at passage 28 onto the chip membrane in the apical side at a density of 300,000 cells/ml and cultured overnight at 37°C without pumping. Following an overnight incubation to facilitate cell attachment to the membrane, medium was perfused through the apical and basolateral channel using a flow rate of 30 µl h^{-1}. The applied flow rate produced a shear stress of 0.00052 dyn/cm^2 to the cells in the apical part, calculated according to the model reported by Oh *et al.* [48]. The Caco-2 cells were cultured under dynamic conditions for 6 days, after which the medium streamed in the apical channel was replaced with medium solution containing the translocation compound. During the translocation exposure the flow rate was increased to 200 µl h^{-1} in order to obtain sufficient aliquots for quantification, but also to decrease

the dead time (time the exposure solution reaches the cells) of the microfluidic assembly . Consequently, an increase in the flow rate led to higher shear stress, determined to be 0.0035 dyn/cm^2, when 200 µl h^{-1} was applied. This increase in the shear stress was still lower than what has been adopted in other microfluidic studies [47] [37] [49]. Furthermore, given the long dead time increased by the outlet tubes as well, the sample collection time-points were extended in concordance with the dead time, followed by sample collection at 24hr exposure. What is more, the dynamic conditions adopted in the microfluidic chip did not allow for determination of mass balance, as previously attempted in the static Transwell systems, due to the constant perfusion of sample in the apical channel. In the dynamic microdevice, the sample collection was done from the outlet tubes for both apical and basolateral channel, at each time point. A correction of the amount measured in the basolateral side was made due to the constant dilution with streamed medium. It is worth-mentioning that the translocation results in the microfluidic chip presented in this study are based on n=1 experiments at one passage, as compared to n=3 experiments performed in Transwells.

4.4.1. ANT translocation assay

The transportation assay was conducted in the microfluidic chip at a working concentration of 1.0 mg/ml. At the chosen perfusion flow rate (200 µl h^{-1}), a good linearity was obtained between the amount of ANT accumulated in the BL channel and the transport time (Figure 10A). Contrary to the BL amount, the amount of ANT in the AP channel showed a short increase, followed by a plateau, indicating that a constant concentration of ANT has reached the AP channel. Furthermore, significantly lower translocation fractions of ANT were noticed in the BL channel, with less than 10% after 24hr perfusion, in contrast with the results obtained in the Transwell inserts, which showed more than 30% translocation in the BL side.

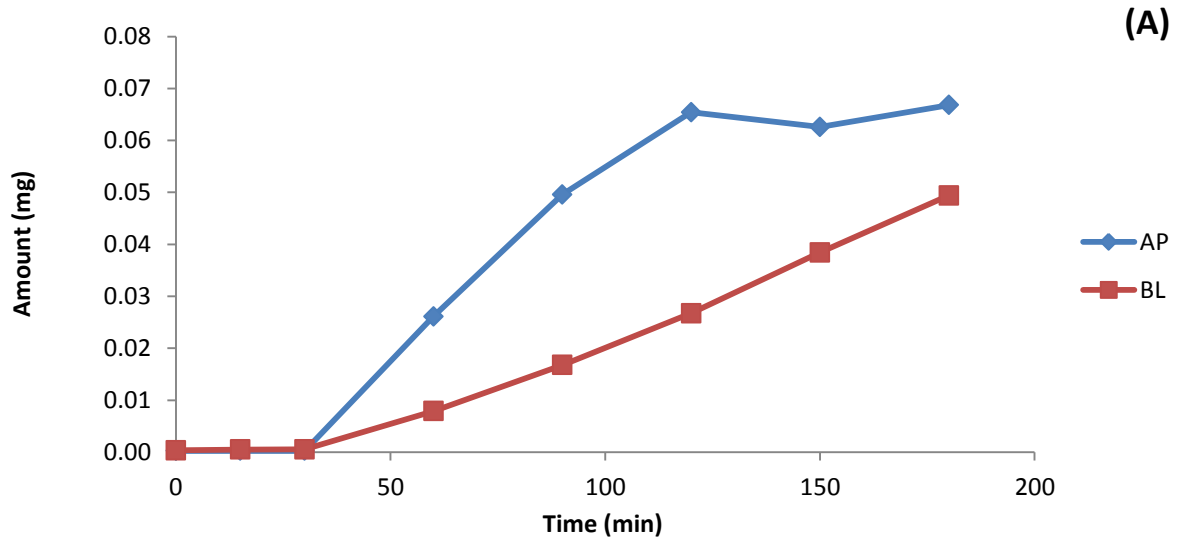

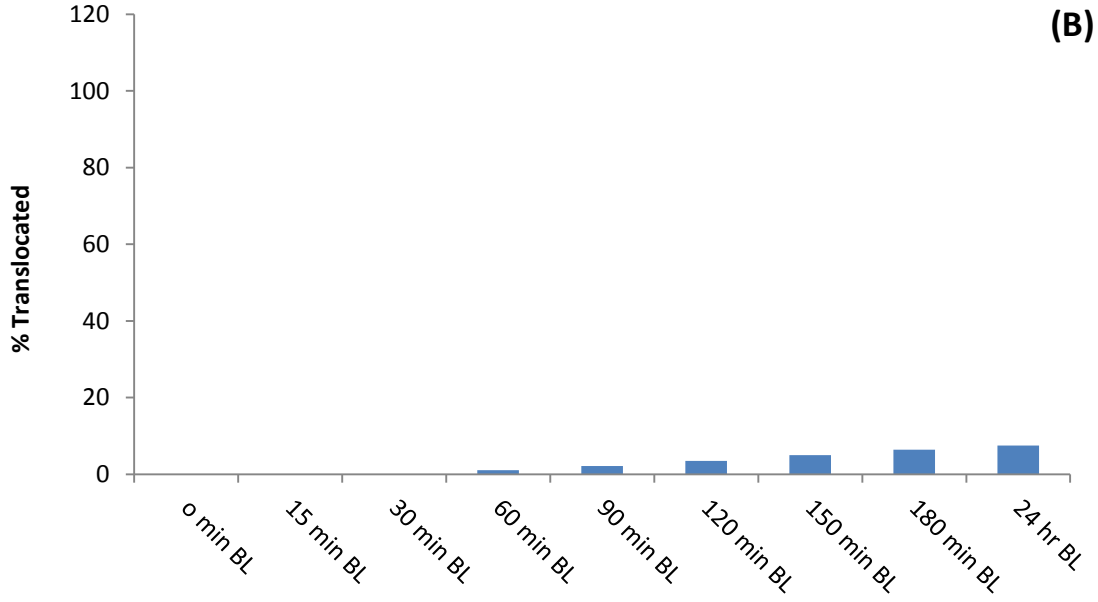

Figure 10: (A) Time course of ANT amount (mg) in the AP (blue) and BL (red) channel of the gut-on-chip device. **(B)** Bar charts representing the percentage of ANT translocated through the Caco-2 monolayer over time in gut-on-chip, measured in the BL (n=1).

Another particular feature observed in the case of the dynamic model is a better linearity in the transport of ANT over time, as compared to the Transwell system. This can be explained by the fact that under static conditions for highly permeable compounds there is build-up of compound that reduces the concentration gradient, thus limiting the flux of the compound. Since the solution is not continuously refreshed, a saturation phenomenon takes place in time. In the case of Transwells, this was indicated by a slight bent in the transport curve of ANT at later time points, showed in Figure 9A (section 4.3.3.). Whereas, in the case of the microfluidic chip, this setup benefited of continuously streamed BL channel that can allow a more linear increase over time, since the BL compartment was constantly refreshed.

4.4.2. LY translocation assay

Given the fact that the microfluidic design did not allow for TEER measurements, the monolayer integrity of the Caco-2 cells cultured on the microfluidic chip was further confirmed by conducting transportation assay of the LY low permeability marker. In this sense, after the 24hr perfusion with ANT, a working medium solution containing 0.5 mg/ml LY was streamed through the upper channel, while the lower channel was constantly perfused with medium. Under these dynamic conditions, the transport of LY in the BL channel was minimal (Figure 11A), with on average 1% of the AP amount translocating through the Caco-2 monolayer (Figure 11B). The minute amounts of LY detected in the BL channel suggested high tight junction integrity of the Caco-2 cells, leading to the conclusion that no cytotoxic effect was exerted by treatment with 1.0 mg/ml ANT. What is more, the permeated fractions of LY were relatively smaller than those found in the Transwell inserts. This made plausible the assumption that the microfluidic

environment can lead to an increase in tight junction integrity. Similar trends in the permeation of LY were also reported by Imura *et al.* [34] where a microfluidic system comprising differentiated Caco-2 cells was compared with the conventional cell culture insert method for LY permeation.

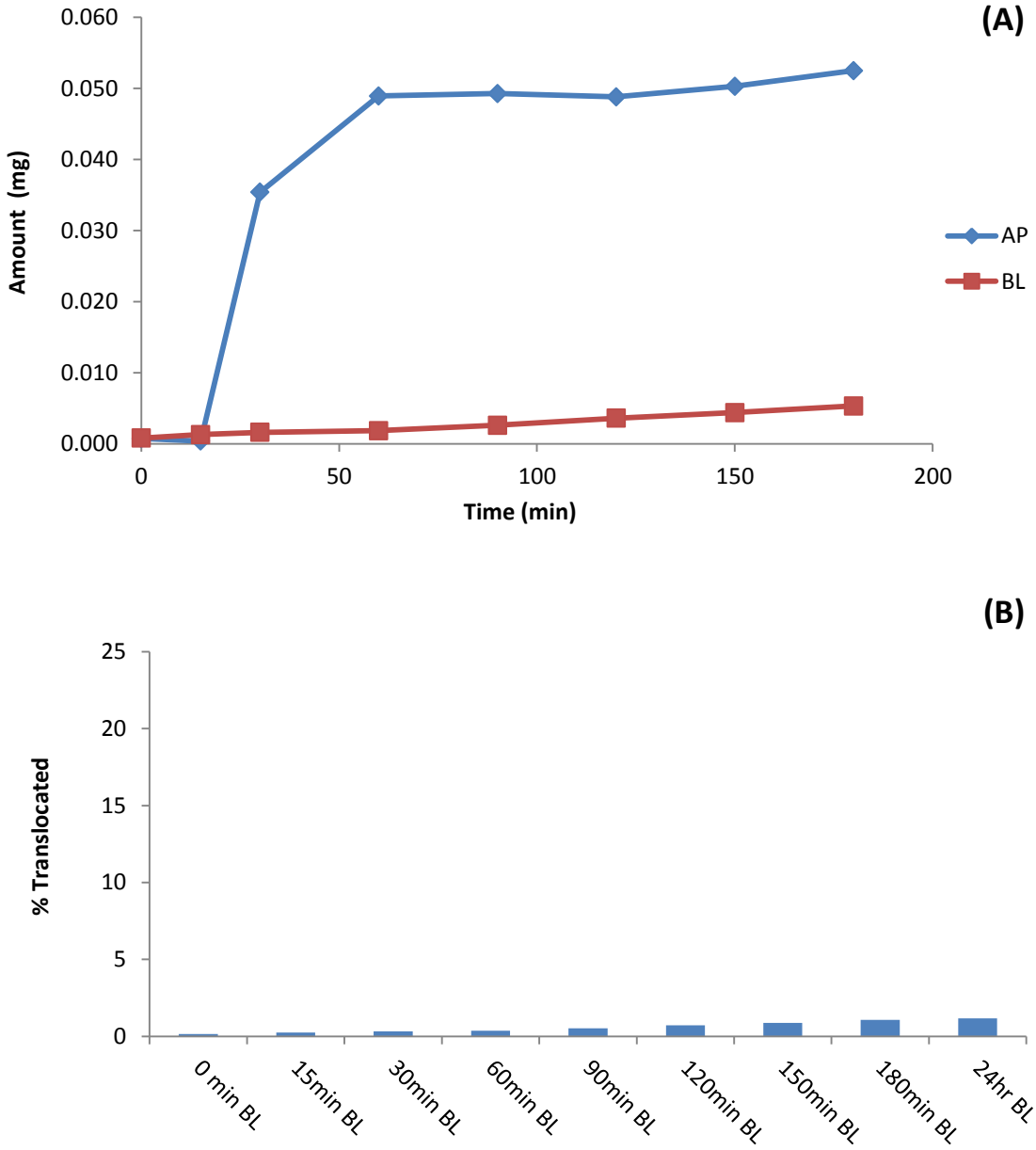

Figure 11: (A) Time course of LY amount in the AP (blue) and BL (red) channel of the gut-on-chip device. **(B)** Bar charts representing the percentage of LY translocated through the Caco-2 monolayer over time in gut-on-chip, measured in the BL part (n=1).

4.5. Permeability correlation Transwell & Gut-on-Chip

Following the permeation assay of ANT and LY low permeability marker, the apparent permeability (P_{app}) was computed for the static and the dynamic Caco-2 *in vitro* models employed in this study. The apparent permeability coefficient is commonly used to characterise the transport of a compound in a two-compartment diffusion model. The flux of the compound was found as the slope of the linear part by plotting the accumulated mass in the BL side relative to the surface area, *versus* time. The corresponding P_{app} (cm s-1) values calculated in the apical-to-basolateral direction for ANT and LY are shown in Figure 12. As far as the apparent permeability coefficient for LY compound is concerned, this showed similar results in both Transwell system and the gut-on-chip, with P_{app} of 0.94 x 10^{-6} cm s^{-1} and 0.60 x 10^{-6} cm s^{-1}, respectively. These results demonstrated that LY is poorly permeable trough the cultured Caco-2 monolayer, denoting a good integrity of the tight junctions when Caco-2 cells were cultured in the static and the dynamic system. In contrast with these results, the permeation of LY in the absence of cells, used as a control, revealed an expectedly high permeability, with a determined P_{app} value of 17.8 x 10^{-6} cm s^{-1}, thus indicating that LY transport was indeed retarded by the formed intestinal barrier. The LY results were also in concordance with data described in literature where permeation of LY was assessed using the cell culture insert method and a microchip system [34]. Their results led to a close approximation of LY P_{app} in both systems, being in agreement with the permeation comparison obtained in this study.

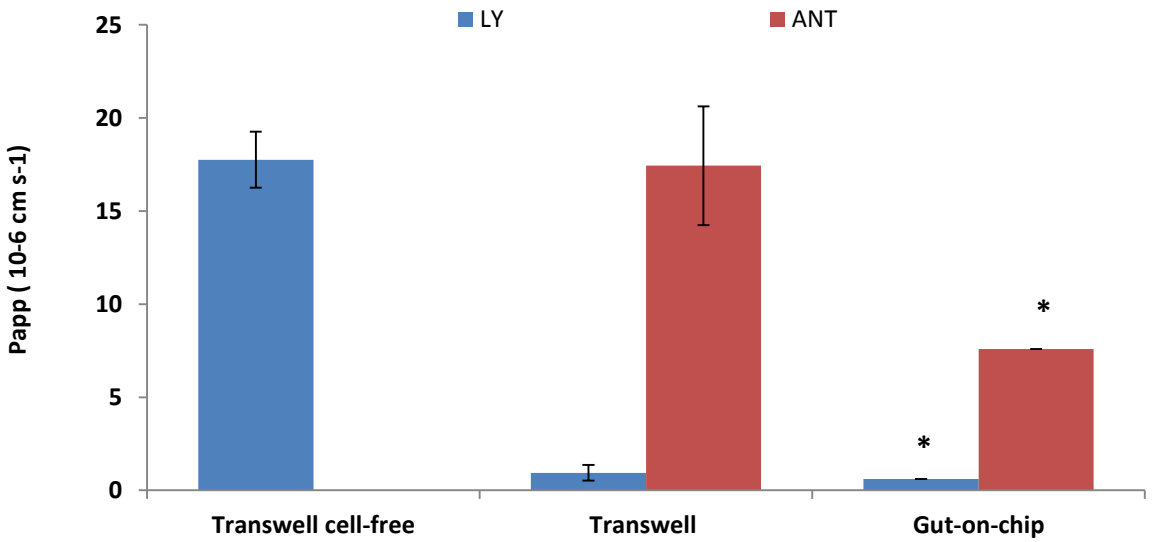

Figure 12: Apparent permeability coefficients (cm s^{-1}) obtained for LY (blue bars) and ANT (red bars) using the gut-on-chip dynamic system and conventional Transwell inserts. For the permeability of LY a control was also performed in the absence of Caco-2 cells. Results presented as mean±SD (n=3). * For the gut-on-chip the results are based on n=1 experiments.

In the case of ANT permeation in the AP-to-BL direction, considerably higher P_{app} values were obtained (Figure 12), characteristic of highly permeable compounds. The P_{app} determined in Transwell inserts revealed higher P_{app} coefficient, 17.4 x 10^{-6} cm s^{-1}, as compared to the 7.59 x 10^{-6} cm s^{-1} P_{app} coefficient determined under the dynamic conditions. According to the classification of drugs' permeability in Caco-2 cells, compounds with measured P_{app} values higher than 1 x 10^{-6} cm s^{-1} are categorized as being highly permeable, while compounds displaying P_{app} under 1 x 10^{-6} cm s^{-1} are considered to have low permeability [34]. From the results obtained for ANT and LY in the two *in vitro* models, a consistency with values reported in literature was noticed.

An interesting aspect, however, was the more obvious difference in the apparent permeability values obtained for ANT in Transwells and gut-on-chip. It has been previously hypothesised that Caco-2 cultured in static models can lead to lower permeability values than those observed *in vivo* [25] [27]. One of the reasons is due to the relatively flat nature of the Caco-2 cells cultured statically; whereas the *in vivo* conditions are known to comprise numerous microvilli structures in the apical part that significantly increase the absorption area. In this sense, it has been previously demonstrated that adapting dynamic conditions with continuous flow producing shear stress stimulates the formation of microvilli structures in Caco-2 cells [47], thus an increase in permeability is expected. A limiting factor for the lower permeability of ANT in gut-on-chip is speculated to come from the incursion of air bubbles in the microchip when medium was changed. This does not only pose a problem to the cells, but also can reduce the area available for the compound to permeate through the monolayer. Apart from this, it is believed that variations in shear stress can lead to changes in the monolayer morphology. In the dynamic experiments presented here the shear stress was much lower (0.00052 dyn/cm^2) than what was implemented in previous investigations (0.02 dyn/cm^2) [47] [34]. An influence in this case is also exerted by the microchip design, which not only impacts the resulting shear stress on the cells but also the diffusion of the translocation compound. Lastly, it is important to mention that the translocation results performed in the gut-on-chip are based on a preliminary experiment, as compared to the Transwell model. Additional replicates in the case of the dynamic model are required in order to have a thorough comparison of the two *in vitro* models. Apart from this, investigations on the effect of different shear stresses on the morphology and consequently the permeation of compounds through the Caco-2 monolayer stand in need for more conclusive results.

5. Conclusion

In this study the translocation efficiency of two *in vitro* cell-based models for the intestinal barrier was assessed. For this, intestinal Caco-2 cells were cultured in conventional static Transwell inserts and a dynamic gut-on-chip microdevice. Translocation was assessed by applying a high permeability compound- ANT, and a low permeability marker- LY to the apical side of differentiated Caco-2 monolayer. The results demonstrated comparable permeability values in the two *in vitro* models with similar transport trends observed for ANT and LY in the apical-to-basolateral direction. As far as the translocation of ANT is concerned, a linear increase of permeability over time was noticed, with high P_{app} computed in both systems. A relatively higher permeability coefficient was noticed in Transwell system- 17.4 x 10^{-6} cm s^{-1}, whereas the permeability coefficient determined under dynamic conditions was 7.59 x 10^{-6} cm s^{-1}. In terms of monolayer integrity, well-formed tight junctions were deduced, based on LY permeation and TEER measurements (only in Transwells). Permeation of LY across Caco-2 monolayers cultured for 21 days (static conditions) and 6 days (dynamic conditions) revealed minute amounts of LY translocating in the basolateral part after a 24hr exposure period, with a permeability coefficient of 0.94x10^{-6} cm s^{-1} in Transwell system, and 0.60 x10^{-6} cm s^{-1} in the gut-on-chip, showing a close resemblance in this sense. These findings support the validity of the microfluidic device investigated, showing comparable results in terms of translocation properties of the gut-on-chip, as compared with the standard Transwell cultures. Moreover, the use of a miniaturized microfluidic chip such as the one described in this study, comprising a constant laminar flow with shear stress exerted on the cells, similarly to the conditions experienced in the human intestine, allowed a shorter culturing time (6 days) for Caco-2 cells. Advantages were also recognized by obtaining a more automatized and controlled conditions for performing permeability screening of drugs, as compared to the static Transwell systems. To this it can be added the minimal consumption of costly reagents, including culture media, drug compounds, and cells, but sufficient aliquots for quantification measurements.

6. Future perspectives

In this study a comparison of two (static and dynamic) *in vitro* models was attempted, evaluating their properties for translocation of ANT and LY. However, this comparison was rather limited given the fact that the translocation studies on the dynamic microdevice were resumed to only a preliminary experiment at this stage. Thus, additional studies performed at different Caco-2 passages are required for a more fair comparison between Transwells and gut-on-chip. Furthermore, extending the translocation evaluation of the gut-on-chip device to other drugs with low and high permeability characteristics, but also with different transport routes across the Caco-2 monolayer can provide a more ample picture of the feasibility of such dynamic *in vitro* model. Bearing in mind these circumstances, the use of the microfluidic gut-on-chip model has the potential to

lay the ground for new investigations on intestinal absorption. One example would be the use of this model with co-cultures, such as Caco-2 and HT-29 (mucus-producing cells). The use of such co-cultures can account for a better representation of the human intestine, as the presence of mucus was demonstrated to exert an influence on the permeability compounds. For instance, it has been reported that compounds undergoing passive permeability were significantly higher in Caco-2/HT-29 co-cultures than in Caco-2 monolayers [20]. A further possibility when such dynamic *in vitro* model is used, as previously described by Kim et al., is also to integrate intestinal microbes for longer periods, feature that is limited in the current static intestinal *in vitro* models [35]. This was shown to improve the intestinal barrier functions. On the same note, the technology of this dynamic microdevice can lead to new studies where the interaction of organs is investigated on-chip. Attempts in this sense were described for intestine-liver models [50] [51].

As far as the design of the microfluidic chip is concerned, this proved to be beneficial in obtaining a constant low fluid flow that refreshes the cells. Apart from this, its miniaturized character proves advantageous for reducing the amounts of reagents used, but also making it less prone to contamination as sometimes it is experienced with static models, given the repeated steps needed to refresh medium. Yet, the incorporation of certain features such on-chip electrodes for direct TEER measurements could facilitate monitoring the integrity of the monolayer. What is more, incorporating direct TEER measurement on chip, as demonstrated in the design proposed by Odij et al, can also provide more insight into the effect of membrane integrity of cells being exposed to different flow rates, consequently different shear stresses, but also as a check for cell viability after exposure to a certain compounds [52]. Areas for improvement also concern the frequent intervention of air bubbles in the chip/capillaries when medium is changed. The presence of air bubbles can prove harmful to the cells and can limit the absorption area on the membrane. A solution to this problem could be the incorporation of air bubble traps at the inlets of the chip. This approach was successfully adopted in the study performed by Imura *et al.* where the incursion of air bubbles in the chip system was prevented by setting up traps made of silicone and teflon tubes at the injection ports [34]. On a final note, although the use of static *in vitro* model, such as Transwells, still remains the main choice for intestinal absorption studies, early work towards the incorporation of dynamic models showed promising potential in this area. The switch towards using microfluidic gut-on-chip devices is believed to become more prominent in the coming years and ultimately to reduce/replace the use of *in vivo* animal models.

Bibliography

[1] S. N. Bhatia and D. E. Ingber, "Microfluidic organs-on-chip," *Nature Biotechnology,* vol. 32, no. 8, pp. 760-772, 2014.

[2] T. Mammoto, A. Mammoto and D. E. Ingber, "Mechanobiology and Developmental Control," *The Annual Review od Cell and Developmental Biology,* no. 29, pp. 27-61, 2013.

[3] D. Huh, Y.-S. Torisawa, G. A. Hamilton, H. J. Kim and D. E. Ingber, "Microengineered physiological biomimicry: Organs-on-Chips," *Lab on Chip,* vol. 12, pp. 2156-2164, 2012.

[4] N. S. Bhise, J. Ribas, V. Manoharan, Y. S. Zhang, A. Polini, S. Massa, M. R. Dokmeci and A. Khademhosseini, "Organ-on-a-chip platforms for studying drug delivery systems," *Journal of Controlled Release,* no. 190, pp. 82-93, 2014.

[5] S. Selimovic, M. R. Dokmeci and A. Khademhosseini, "Oragans-on-a-chip for drug discovery," *Current Opinion in Pharmacology,* no. 13, pp. 829-833, 2013.

[6] M. H. Abraham, Y. H. Zhao, J. Le, A. Hersey, C. N. Luscombe, D. P. Reynolds, G. Beck, B. Sherborne and I. Cooper, "On the mechanism of human intestinal absorption," *European Journal of Medicinal Chemistry,* no. 37, pp. 595-605, 2002.

[7] C. H. Versantwoort, C. J. Rompelberg and A. J. Sips, "Methodologies to Study Human Intestinal Absorption. A review," RIVM, Bilthoven, 2000.

[8] P. V. Balimane and C. Saeho, "Cell culture-based models for intestinal permeability: a critique," *Drug Discovery Today,* vol. 10, no. 5, pp. 335-343, 2005.

[9] C. A. Bailey, P. Bryla and A. W. Malick, "The use of intestinal epithelial cell culture model, Caco-2, in pharmaceutical development," *Advanced Drug Delievery Reviews,* no. 22, pp. 85-103, 1996.

[10] K. L. Audus, R. L. Bartel, I. J. Hidalgo and R. T. Borchardt, "The Use of Cultured Epithelail and Endothelial Cells for Drug Transport and Metabolism Studies," *Pharmaceutical Research,* vol. 7, no. 5, pp. 435-451, 1990.

[11] S. Yamashita, T. Furubayashi, M. Kataoka, T. Sakane, H. Sezaki and H. Tokuda, "Optimized conditions for prediction of intestinal drug permeability using Caco-2 cells," *European Journal of Pharmaceutical Sciences,* no. 10,

pp. 195-204, 2000.

[12] A. Quaroni and J. Hochman, "Development of intestinal cell culture models for drug transport and metabolism studies," *Advanced Drug Delievery Reviews,* no. 22, pp. 3-52, 1996.

[13] P. Artursson, "Cell cultures as models for drug absorption across the intestinal mucosa," *Critical Reviews in Therapeutic Drug Carrier Systems,* vol. 8, no. 4, pp. 305-330, 1991.

[14] R. van Breemen and Y. Li, "Caco-2 cell permeability assays to measure drug absorption," *Expert Opinion on Drug Metabolism & Toxicology,* vol. 1, no. 2, pp. 175-185, 2005.

[15] G. Wilson, I. F. Hassan, C. J. Dix, I. Williamson, R. Shah, M. Mackay and P. Artursson, "Transport and Permeability Properties of Human Caco-2 Cells: an In Vitro Model of the Intestinal Epithelial Cell Barrier," *Journal of Controlled Release,* no. 11, pp. 25-40, 1990.

[16] W. Rubas, N. Jezyk and G. M. Grass, "Comparison of the Permeability Characteristics of a Human Colonic Epithelial (Caco-2) Cell Line to Colon of Rabbit, Monkey, and Dog Intestine and Human Drug Absorption," *Pharmaceutical Research,* vol. 10, no. 1, pp. 113-118, 1993.

[17] P. Artursson, "Epithelial Transport of Drugs in Cell Culture. I: A Model For Studying The Passive Diffusion Of Drugs Over Intestinal Absorptive (Caco-2) Cells," *Jornal of Pharmaceutical Sciences,* vol. 79, no. 6, pp. 476-482, 1990.

[18] A.-L. B. Ungell, "Caco-2 replace or refine?," *Drug Discovery Today: Technologies,* vol. 1, no. 4, pp. 423-430, 2004.

[19] A. Wikman, J. Karlsson, I. Carlstedt and P. Artursson, "A Drug Absorption Model Based on the Mucus Layer Producing Human Intestinal Goblet Cell line HT29-H," *Pharmaceutical Research,* vol. 10, no. 6, pp. 743-752, 1993.

[20] C. Hilgendorf, H. Spahn-Langguth, C. G. Regardh, E. Lipka, G. L. Amidon and P. Langguth, "Caco-2 versus caco-2/HT29-MTX co-cultured cell lines: Permeabilities via diffusion, inside- and outside-directed carrier-mediated transport," *Journal of Pharmaceutical Sciences,* pp. 63-75, 2000.

[21] E. S. Rodansky, L. A. Johnson, J. R. Spence and P. D. Higgins, "Intestinal organoids: A model of intestinal fibrosis for evaluating anti-fibrotic drugs," *Experimental and Molecular Pathology,* no. 98, pp. 346-351, 2015.

[22] S. Date and T. Sato, "Mini-Gut Organoids: Reconstitution of the Stem Cell Niche," *Annual Review of Cell and Developmental Biology,* no. 31, pp. 269-

289, 2015.

[23] Y. Sambuy, I. De Angelis, G. Ranaldi, M. L. Scarino, A. Stammati and F. Zucco, "The Caco-2 cell line as a model of the intestinal barrier: influence of cell and culture-related factors on Caco-2 cell functional characteristics," *Cell Biology and Toxiciology,* no. 21, pp. 1-26, 2005.

[24] Brunswick Laboratories, "Clinical/Preclinical Testing & Research for Phytonutrients," 2013. [Online]. Available: http://www.brunswicklabs.com/pharmaceutics/adme/tox/caco-2-permeability-screening. [Accessed 20 May 2016].

[25] P. Artursson and R. T. Borchardt, "Intestinal Drug Absorption and Metabolism in Cell Cultures: Caco-2 and Beyond," *Pharmaceutical Research,* vol. 14, no. 12, pp. 1655-1658, 1997.

[26] A. B. Thomson and J. M. Dietchy, "The Role of the Unstirred Water Layer in Intestinal Permeation," *Experimental Pharmacology,* pp. 165-269, 1984.

[27] I. J. Hidalgo, K. M. Hillgren, G. M. Grass and R. T. Borchardt, "Characterization of the Unstirred Water Layer in Caco-2 Cell Monolayers Using a Novel Diffusion Apparatus," *Pharmaceutical Research,* vol. 8, no. 2, pp. 222-227, 1991.

[28] P. Artursson, K. Palm and K. Luthman, "Caco-2 monolayers in experimental and theoretical predictions of drug transport," *Advanced Drug Delivery Reviews,* no. 22, pp. 67-84, 1996.

[29] W. I. Lencer, C. Delp, M. R. Neutra and J. L. Madara, "Mechanism of Cholera Toxin Action on a Polarized Human Intestinal Epithelial Cell Line: Role of Vesicular Traffic," *J Cell Biology,* vol. 6, no. 117, pp. 1197-1209, 1992.

[30] M. Jodal, S. Holmgren, O. Lundgren and A. Sjoqvist, "Involment of the Myentric Plexus in the Cholera Toxin-Induced Ne Fluid Secretion in the Rat Small Intestine," *Gastroenterology,* no. 105, pp. 1286-1293, 1993.

[31] P. Anderle, E. Niederer, W. Rubas, C. Hilgendorf, H. Spahn-Langguth, H. Wunderli-Allenspach, H. P. Merkle and P. Langguth, "P-Glycoprotein (P-gp) Mediated Effflux in Caco-2 Cell Monolayers: The Influence of Culturing Conditions and Drug Exposure on P-gp Expression Levels," *Journal of Pharmaceutical Sciences,* vol. 6, no. 87, pp. 757-762, 1998.

[32] S. Selimovic, M. R. Dokmeci and A. Khademhosseini, "Organs-on-a-chip for drug discovery," *Current Opinion in Pharmacology,* no. 13, pp. 829-833, 2013.

[33] J. P. Wikswo, E. L. Curtis, Z. E. Eagleton, B. C. Evans, A. Kole, L. H. Hofmeister and W. J. Matloff, "Scaling and systems biology for integrating multiple organs-on-a-chip," *Lab on a Chip,* vol. 181, no. 13, pp. 3496-3511, 2013.

[34] Y. Imura, Y. Asano, K. Sato and E. Yoshimura, "A Microfluidic System to Evaluate Intestinal Absorption," *Analytical Sciences,* no. 25, pp. 1403-1407, 2009.

[35] H. J. Kim, D. Huh, G. Hamilton and D. E. Ingber, "Human gut-on-a-chip inhabitated by microbial flora that experiences intestinal peristalsis-like motions and flow," *Lab on a chip,* no. 12, pp. 2165-2174, 2012.

[36] Q. Ramadan, H. Jafarpoorchekab, C. Huang, P. Silacci, S. Carrara, G. Koklu, J. Ghaye, J. Ramsden, C. Ruffert, G. Vergeres and M. A. Gijs, "NutriChip: nutrion analysis meets microfluidics," *Lab on a Chip,* vol. 2, no. 13, pp. 196-203, 2013.

[37] H. Kimura, T. Yamamoto, H. Sakai, Y. Sakai and T. Fujii, "An integrated microfluidic system for long-term perfusion culture and on-line monitoring of intestinal tissue models," *Lab Chip,* no. 8, pp. 741-746, 2008.

[38] T. Ogihara, I. Tamai and A. Tsuji, "Application of Fractal Kinetics for Carrier-Mediated Transport of Drugs Across Intestinal Epithelial Membrane," *Pharmaceutical Researcg,* vol. 4, no. 15, pp. 620-625, 1998.

[39] O. Lacombe, J. Woodley, C. Solleux, J.-M. DElbos, C. Boursier-Neyret and G. Houin, "Localisation of drug permeability along the rat small intestine, using markers of the paracellular, transcellular and some transporter routes," *European Journal of Pharmaceutical Sciences,* no. 23, pp. 375-391, 2004.

[40] M. Lemieux, F. Bourchard, P. Gosselin, J. Paquin and M. A. Mateescu, "The NCI-N87 cell line as a gastric epithelial barrier model for drug permeability assay," *Bioechemical and Biophysical Communications,* vol. 412, no. 3, pp. 429-434, 2011.

[41] J. Jakubikova, J. Sedlak, R. Mithen and Y. Bao, "Role of PI3K/AKT and MEK/ERK signaling pathways in sulforaphane- an erucin-induced phase II enzymes and MRP2 transcription, G2/M arrest and cell death in Caco-2 cells," no. 69, pp. 1543-1552, 2005.

[42] H. Li, B. van Ravenzwaay, I. M. C. M. Rietjens and J. Louisse, "Assessment of an in vitro transport model using BeWo b30 cells to predict placental transfer of compounds," *Toxicokinetics and Metabolism,* no. 87, pp. 1661-1669, 2013.

[43] International Conference on Harmonization (ICH) of Technical Requirements for the Registration of Pharmaceuticals for Human Use, "Validation of analytical procedures: Text and Methodology," Geneva, 1996.

[44] T. Mukherjee, E. Squillantea, M. Gillespieb and J. Shao, "Transepithelial Electrical Resistance is Not a Reliable Measurement of the Caco-2 Monolayer Integrity in Transwell," *Drug Delivery,* vol. 1, no. 11, pp. 11-18, 2008.

[45] R. Konsoula and F. A. Barile, "Correlation of in vitro cytotoxicity with paracellular permeability in Caco-2 cells," *Toxicology in Vitro,* no. 19, pp. 675-684, 2005.

[46] R. Saitoh, K. Sugano, N. Takata, T. Tachibana, A. Higashida, Y. Nabuchi and Y. Aso, "Correction of Permeability with Pore Radius of Tight Junctions in Caco-2 Monolayers Improves the Prediction of the Dose Fraction of Hydrophilic Drugs Absorbed by Humans," vol. 21, no. 5, pp. 749-755, 2004.

[47] H. J. Kim and D. E. Ingber, "Gut-on-a-Chip microenvironment induces human intestinal cells to undergo villus differentiation," *Integrative Biology,* vol. 9, no. 5, pp. 1130-1140, 2013.

[48] S. W. Oh, K. Lee, B. Ahn and E. P. Furlani, "Design of pressure-driven microfluidic networks using electric circuit analogy," *Lab on a Chip,* vol. 12, pp. 515-545, 2012.

[49] M. Chi, B. Yi, S. Oh, D.-J. Park, J. H. Sung and S. Park, "A microfluidic cell culture device (μFCCD) to culture epithelial cells with physiological and morphological properties that mimic those of the human intestine," vol. 58, no. 17, pp. 1-10, 2015.

[50] T. Bricks, P. Paullier, A. Legendre, M.-J. Fleury, P. Zeller, P. Franck, P. M. Anton and E. Leclerc, "Development of a new microfludic platform integrating co-cultures of intestinal and liver cell lines," *Toxicology in Vitro,* no. 28, pp. 885-895, 2014.

[51] H. Kimura, T. Ikeda, H. Nakayama, Y. Sakai and T. Fujii, "An On-Chip Small Intestine-Liver Model For Pharmacokinetic Studies," *Journal of Automation,* vol. 20, no. 3, pp. 265-273, 2015.

[52] M. Odijk, A. D. van der Meer, D. Levner, H. Jung Kim, M. W. van der Helm, L. I. Segerink, J.-P. Frimat, G. A. Hamilton, D. E. Ingber and A. van den Berg, "Measuring direct current tans-epithelial electrical resistance in organ-on-a-chip microsystems," no. 15, pp. 745-752, 2015.

Appendices

Appendix 1, Microchip dimensions

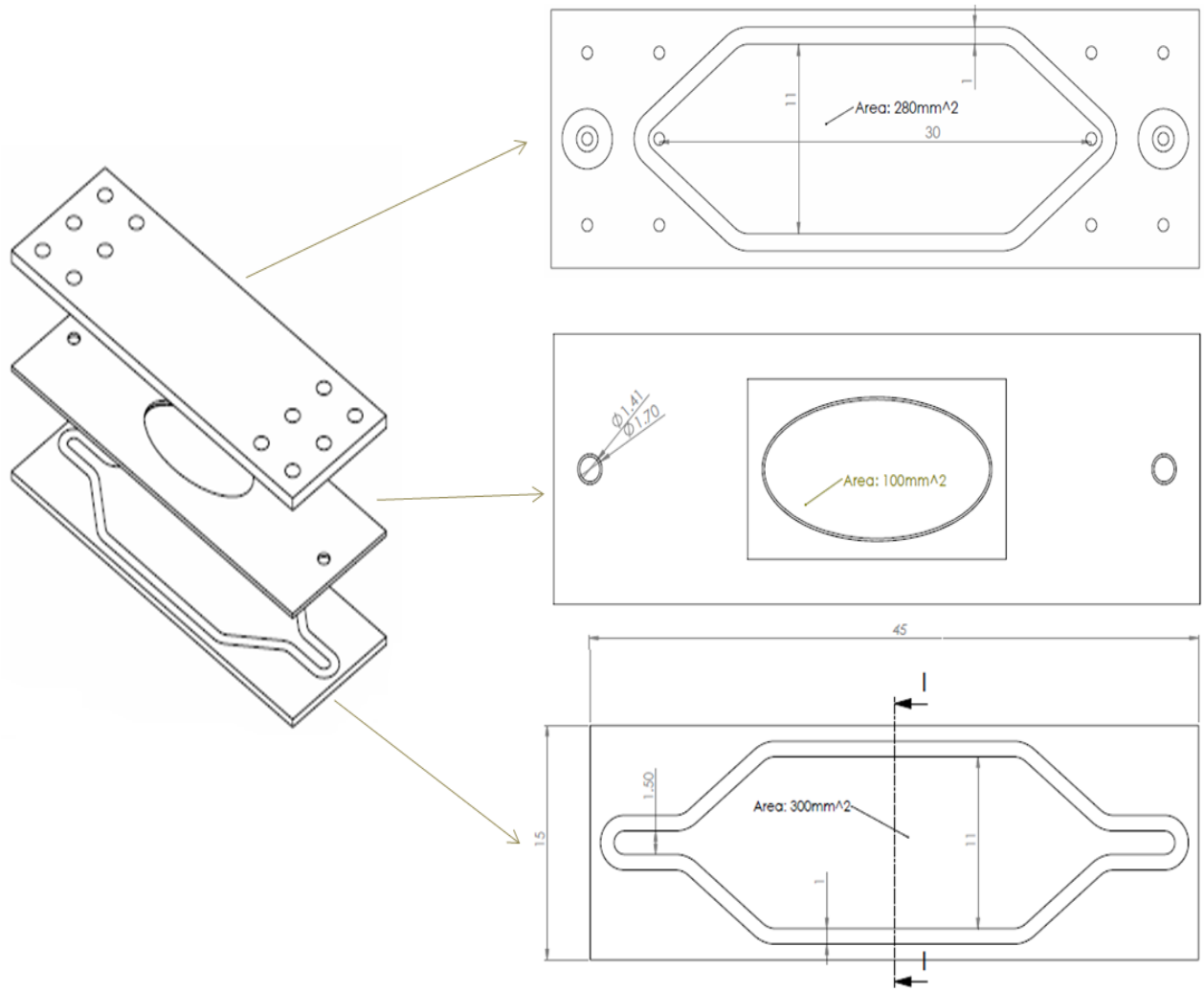

Figure 13: Schematic of the microchip assembly, consisting of two reseable glass slides (top and bottom) and a polyester porous membrane sandwiched between the slides. The dimensions for each component are portrayed.

Appendix 2, ANT recovery & stability

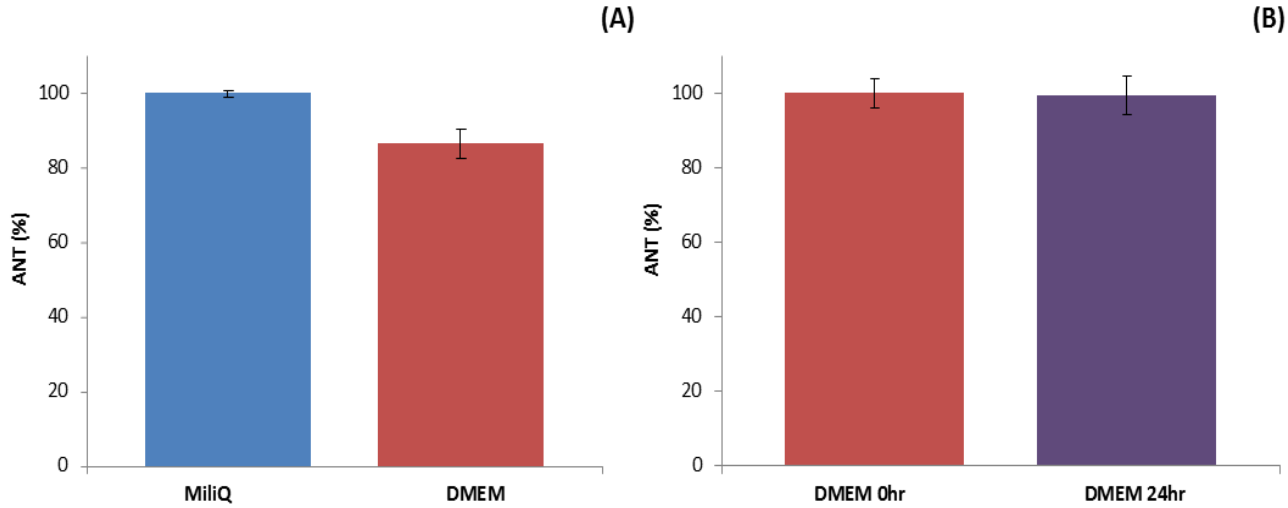

Figure 14: (A) Recovery of ANT (0.1 mg/ml) after protein precipitation in DMEM (red bar), relative to preparation in MiliQ (blue bar). **(B)** ANT stability following 24hr incubation at 37°C (purple bar) in comparison to the initial stock prepared in DMEM (red bar). Results presented as mean±SD (n=3).

Appendix 3, LY calibration line

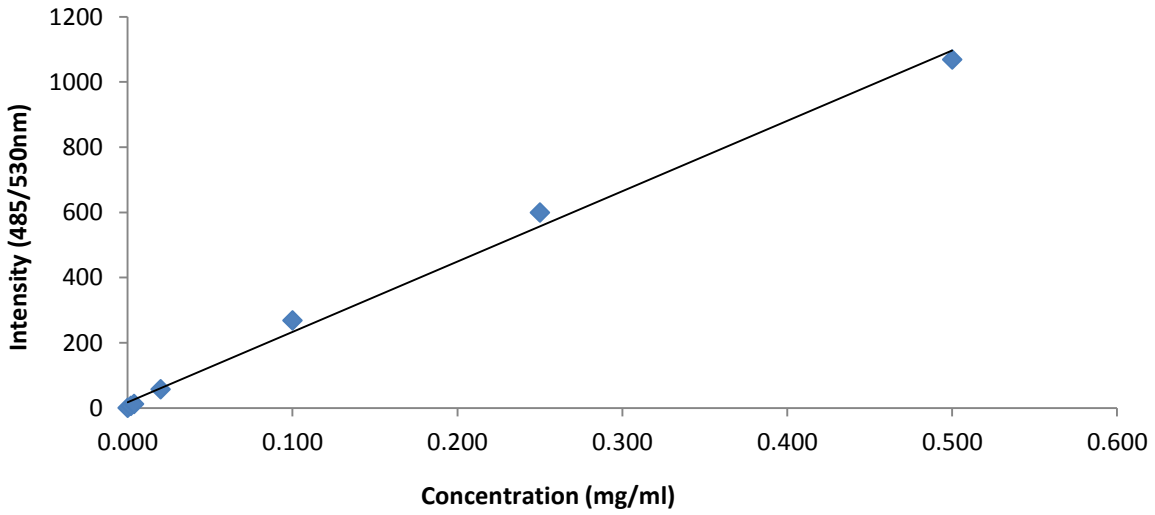

Figure 15: LY calibration graph (n=3) plotting the concentration (mg/ml) against the fluorescence intensity (485/530 nm) in the 0.002-0.5 mg/ml range. A correlation coefficient (r^2) of 0.9954 was obtained, denoting a good linearity of the calibration graph.

Appendix 4, LY translocation cell-free Transwell

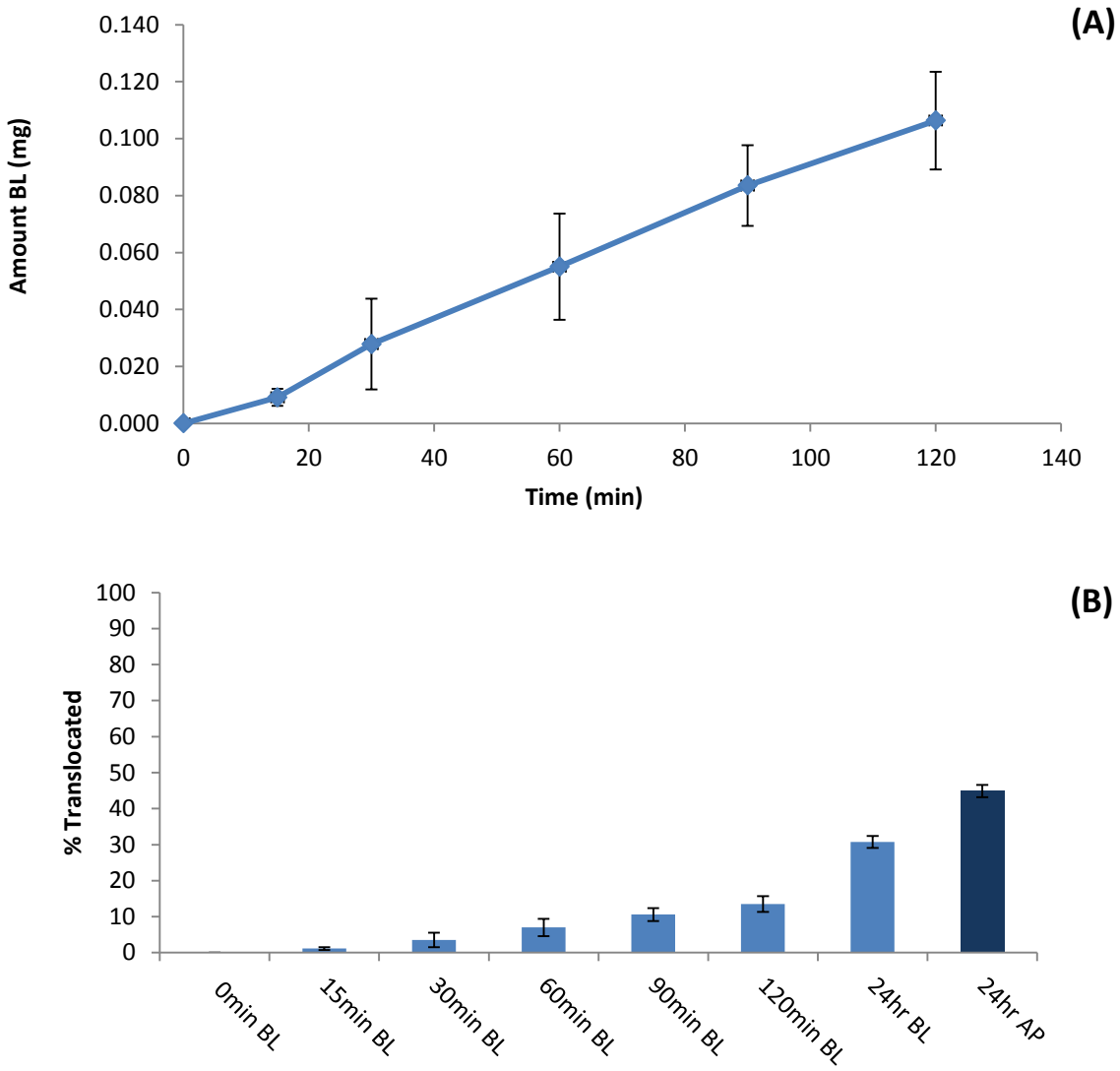

Figure 16: (A) LY transport in the apical-to-basolateral direction measured over a span of 120 min. **(B)** Bar charts representing the percentage of LY translocated through the Caco-2 monolayer over time in cell-free Transwell inserts in the BL part (light blue bars), and the remaining percentage of LY compound in the AP side after 24hr exposure (dark blue bars). Data computed as mean±SD (n=3) (see Appendix 3 for LY calibration line).